THE CLEVELAND CLINIC FOUNDATION

DEPARTMENT OF ARTIFICIAL ORGANS
CLINIC CENTER, CLEVELAND OHIO 44106

DISCLAIMER

COO-2208-4

AVAILABLE SPACE FOR A TOTALLY IMPLANTABLE CARDIAC PROSTHESIS

PROGRESS REPORT

THE CLEVELAND CLINIC FOUNDATION
DEPARTMENT OF ARTIFICIAL ORGANS

April 1, 1973 - July 31, 1973

PREPARED FOR THE U.S. ATOMIC ENERGY COMMISSION
UNDER CONTRACT AT(11-1)-2208

TABLE OF CONTENTS

1.0 ABSTRACT

The goal of the present program is to define the spatial constraints of the body for a totally implantable cardiac prosthesis. The design is such that the prosthesis is compatible with both the human and the experimental animal, the calf.

Most recent efforts were directed to the definition of the size and shape of the human thorax for implanting the blood pump. This was done by formulating a mathematical shape model from dimensions obtained from plastic molds made in the chest cavity of human cadavers. The shape model was used in conjunction with dimensions obtained from 100 chest radiographs of living humans to arrive at a statistical distribution of chest dimensions.

The results are presented as scale drawings of the walls of the thorax as a function of the percent of the population having sizes smaller than the given curves. An effort is underway to define the natural heart boundaries in the chest to define soft tissue and vascular connections in the thorax.

A parallel effort was to determine the anatomical and physiological tolerance of calves to implanted models of the thermal converter. Five calves were implanted with models, four have been sacrificed at 8 to 12 months after implantation, and one remains under observation. All calves were in good physical condition with the retroperitoneal infrarenal space appearing to be most feasible.

2.0 STATEMENT OF EFFORTS

Dr. Y. Nosé, the Principal Investigator has devoted approximately ten percent of his time to this contract. This same level of effort is anticipated for the remainder of the contract period.

ACKNOWLEDGEMENT

The following inaividuals contributed to the efforts reported in this document:

Agishi, T.

Jacobs, G.

Kiraly, R.

Louie, R.

Nosé, Y.

Panke, T.

Picha, G.

Sudilovsky, O.

Urzua, J.

3.0 PROGRESS IN THIS REPORTING PERIOD

Since the last report[1] the major effort was directed in two areas. The first was to continue to define the size and shape of the human thorax for implantation of the blood pump. The second area was to determine the anatomical and physiological tolerance of calves to implants of models of the thermal converter. Both these efforts are described in detail in the following sections.

The definition of the human thorax is virtually complete in regard to the chest wall. Data regarding the natural heart shape and location has already been taken from radiographs but this data has not as yet been processed or analyzed. Soft structure definition should be completed in the next several months to complete the effort to define the thorax.

Four of the five calves with implanted models have been sacrificed while one is still under observation after 12 months. No animal had physical disorder due to the implant.

3.1 DEFINITION OF THE HUMAN THORAX

The purpose of this work is to define the chest cavity of an adult human. This effort is only the first stage in accomplishing the ultimate goal, that of defining not only the chest cavity, but the relative location of pertinent soft structures within this cavity, in the human.

---

1. COO-2208-3. Annual Technical Progress Report on "Available Space For A Totally Implantable Cardiac Prosthesis", July 1, 1972 to March 31, 1973.

In order to determine the mean dimensions for design of the blood pump, a special technique has been developed.

A shape model was made from data taken from transversely sectioned molds of the chest cavity of human cadavers. The normalized shape and curvature of the human chest cavity was determined by analysis of this data on a computer.

The shape model was then combined with the measurements of dimensions on a large number of human plane chest radiographs to determine a distribution of the size of the chest cavity as a function of the percentage of the population having these dimensions.

The ultimately developed technique of the modeling and analysis is also expected to be applicable to clinical cases of artificial heart implantation where standard chest radiographs of the proposed recipient will insure that the prosthesis will fit in the particular patient.

3.1.1 Generation of Model

A detailed description of the essential concepts in the model development is included in the previous report (COO-2208-3). Briefly, models generated from molds cast in cadaver thorax cavities were used to determine chest wall curvature after individual size variations had been normalized out of the data. Nine mold models have been analyzed and the resulting data used to generate a preliminary vertically dependent model. This model consists of a normalized curve for each quadrant (i.e. left anterior, left posterior, etc.) at a known level in the thorax. The vertical level under investigation is specified in terms of the percent vertical distance between two reference points identifiable on the

radiograms. Because the individual vertebra were not distinct in the films, these reference points are specified in terms of rib number and certain x-ray dimensions. They are located roughly at the T4 and T10 regions of the chest. A typical normalized curve is shown in Figure 1. This curve represents the model ($\pm$ 1 standard deviation) for the left anterior portion of a transverse section at approximately the T10 region. Data for this curve is shown at the top of Table 1 under "Left Anterior". Comparison of Figure 1 with Figure 2 demonstrates graphically the reduction in error when a vertically dependent model is used. Data for the T6 and T4 regions is shown in Tables 2 and 3, respectively. A comparison of the left and right anterior and posterior sections of all model data averaged in the vertical direction is shown in Figures 3 and 4 and clearly demonstrates symmetry of the thoracic wall shape.

Example of Model Use. Assume the Atlas projections shown in Figure 5 and 6 represent the actual structure of a patient under investigation for a possible prosthesis. The transverse section shown in Figure 5 is labeled with a set of axis determined by one reference point on the vertebral column and another on the distal point of the inner side of the sternum. The dimensions A, B, and C represent those measurements of the chest cavity visible on the radiogram. These simulated x-ray dimensions are shown at the top of Table 4 as A', B', and C'. Assuming T10 region of the symmetrical model is used, x-y coordinates of the predicted thorax are generated by simple multiplication; i.e., for the left anterior quadrant, the normalized x values (X_n) are multiplied by C', and the normalized y values (Y_n) by B'. The total predicted curve for this

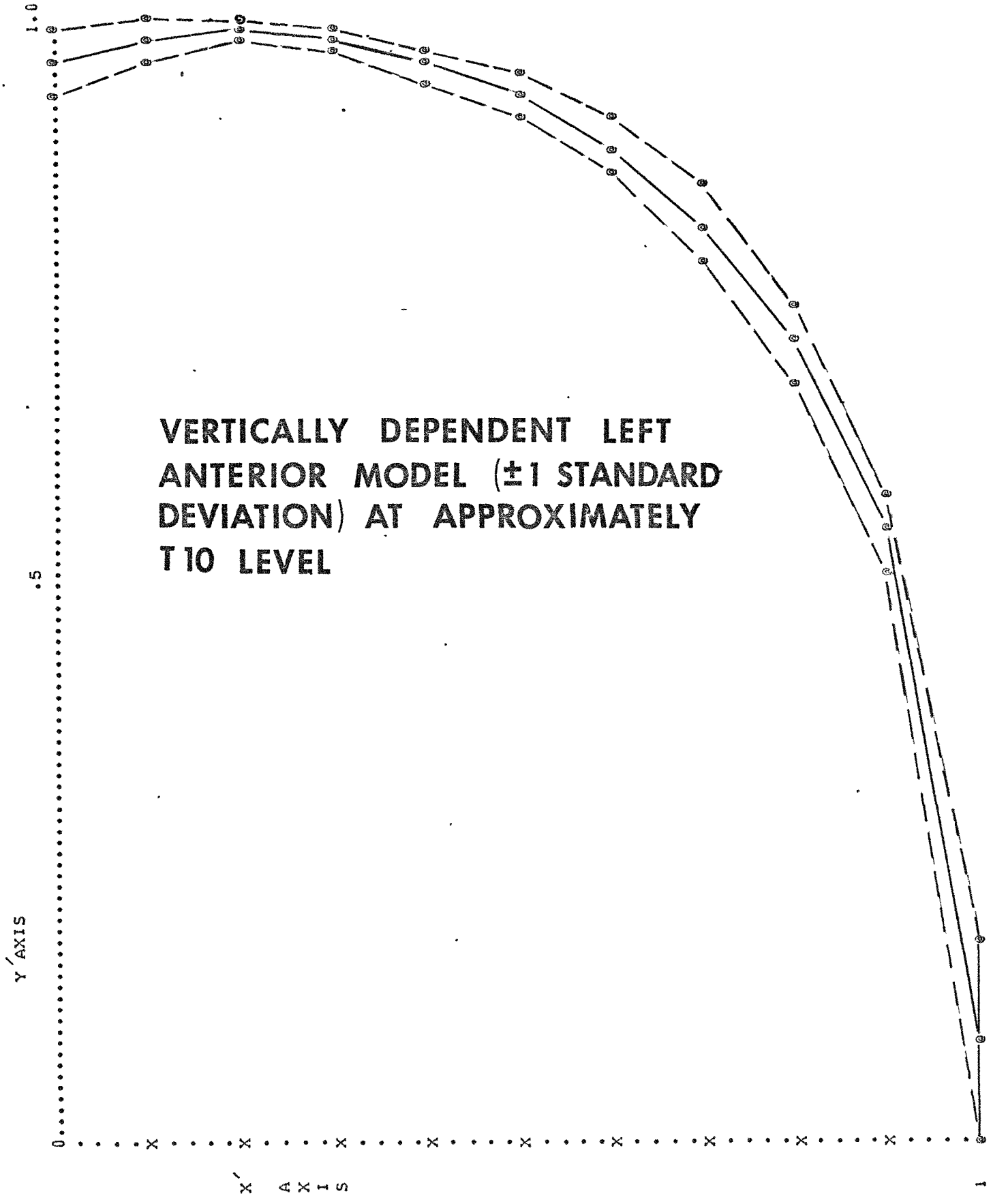
1.0
.5
0
Y AXIS
X AXIS
1
VERTICALLY DEPENDENT LEFT ANTERIOR MODEL (±1 STANDARD DEVIATION) AT APPROXIMATELY T 10 LEVEL

FIG. 1

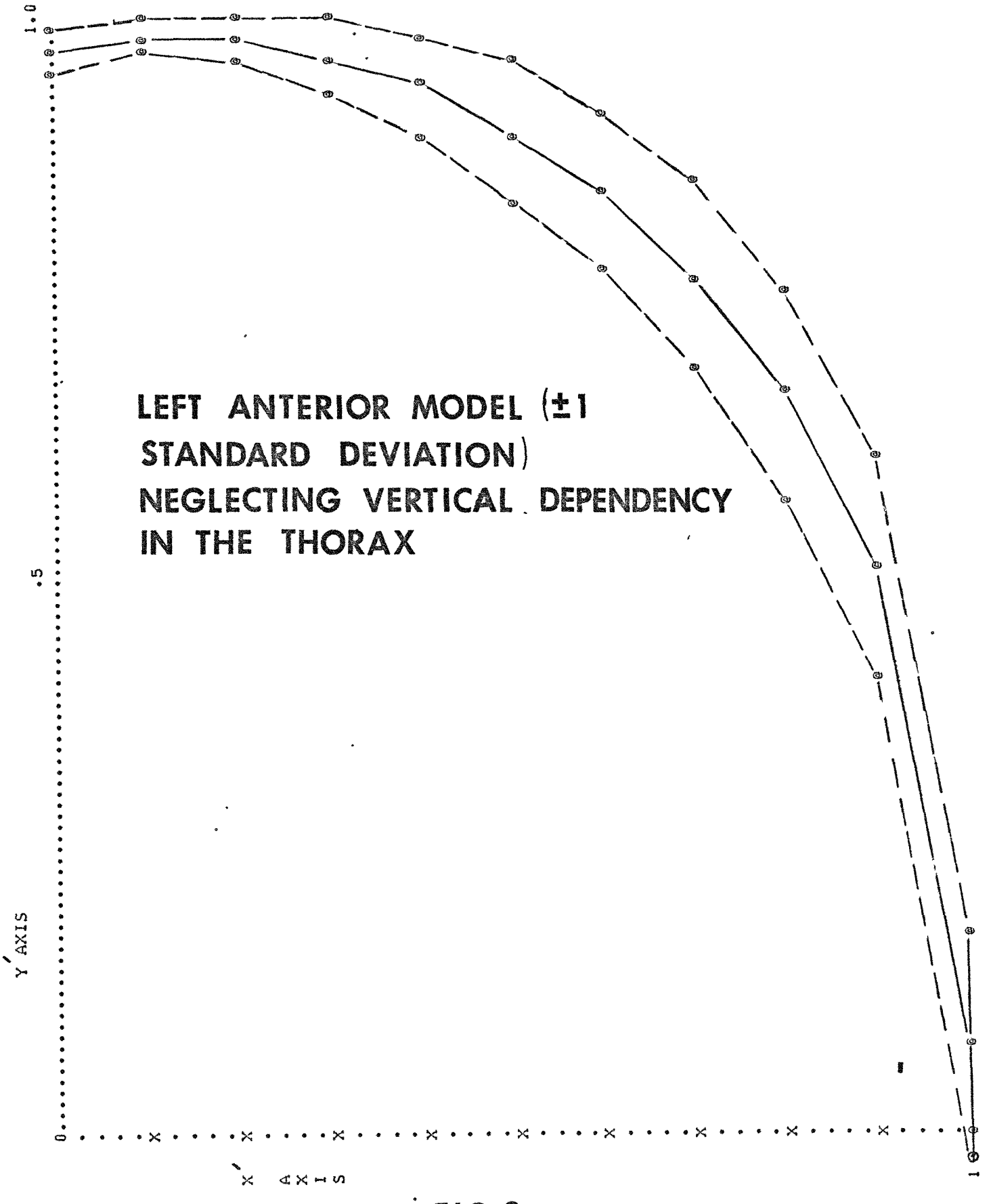
1.0
.5
0
Y AXIS
X AXIS
1
LEFT ANTERIOR MODEL (±1 STANDARD DEVIATION) NEGLECTING VERTICAL DEPENDENCY IN THE THORAX

FIG. 2

FROM SPEC. # 3.00TO SPEC. # 9.00
LEFT SIDE
ANTERIOR
SLICES USED IN AVERAGE= 7.00

XINT	AVG	STDEV	PRCT
0.0000	0.9714	0.0294	3.0232
0.1000	0.9898	0.0162	1.6386
0.2000	0.9959	0.0090	0.9022
0.3000	0.9854	0.0100	1.0120
0.4000	0.9683	0.0154	1.5853
0.5000	0.9405	0.0217	2.3124
0.6000	0.8935	0.0254	2.8388
0.7000	0.8210	0.0341	4.1592
0.8000	0.7162	0.0337	4.7054
0.9000	0.5468	0.0368	6.7384
1.0000	0.0830	0.0776	93.5512

FROM SPEC. # 3.00TO SPEC. # 9.00
LEFT SIDE
POSTERIOR
SLICES USED IN AVERAGE= 7.00

XINT	AVG	STDEV	PRCT
0.0000	0.0000	0.0000	0.0000
0.1000	0.1205	0.0393	32.6445
0.2000	0.4850	0.0917	18.8985
0.3000	0.8028	0.1063	13.2380
0.4000	0.9365	0.0690	7.3718
0.5000	0.9943	0.0213	2.1380
0.6000	0.9829	0.0207	2.1020
0.7000	0.9160	0.0555	6.0549
0.8000	0.7562	0.1029	13.6086
0.9000	0.4579	0.1685	36.8046
1.0000	0.0000	0.0000	0.0000

FROM SPEC. # 3.00TO SPEC. # 9.00
RIGHT SIDE
ANTERIOR
SLICES USED IN AVERAGE= 7.00

XINT	AVG	STDEV	PRCT
0.0000	0.9830	0.0156	1.5822
0.1000	0.9931	0.0064	0.6487
0.2000	0.9972	0.0032	0.3193
0.3000	0.9944	0.0043	0.4319
0.4000	0.9768	0.0109	1.1173
0.5000	0.9400	0.0145	1.5403
0.6000	0.8886	0.0186	2.0965
0.7000	0.8105	0.0365	4.5040
0.8000	0.6987	0.0586	8.3813
0.9000	0.5177	0.0687	13.2673
1.0000	0.0215	0.0367	171.1594

FROM SPEC. # 3.00TO SPEC. # 9.00
RIGHT SIDE
POSTERIOR
SLICES USED IN AVERAGE= 7.00

XINT	AVG	STLEV	PRCT
0.0000	0.0000	0.0000	0.0000
0.1000	0.0713	0.0323	45.2526
0.2000	0.4645	0.0544	11.7165
0.3000	0.8219	0.0456	5.5459
0.4000	0.9469	0.0206	2.1800
0.5000	0.9886	0.0076	0.7655
0.6000	0.9796	0.0215	2.1974
0.7000	0.9111	0.0346	3.8002
0.8000	0.7611	0.0513	6.7410
0.9000	0.4734	0.0987	20.8559
1.0000	0.0010	0.0010	0.0006

VERTICALLY DEPENDENT MODEL AT T10 REGION

TABLE 1

FROM SPEC. # 1.00TO SPEC. # 9.00
LEFT SIDE
ANTERIOR
SLICES USED IN AVERAGE= 9.00

XINT	AVG	STDEV	PRCT
0.0000	0.9801	0.0189	1.9326
0.1000	0.9961	0.0162	1.6256
0.2000	1.0020	0.0172	1.7123
0.3000	0.9884	0.0244	2.4677
0.4000	0.9583	0.0349	3.6409
0.5000	0.9154	0.0480	5.2387
0.6000	0.8604	0.0604	7.0142
0.7000	0.7839	0.0731	9.3211
0.8000	0.6852	0.0871	12.7052
0.9000	0.5318	0.0971	18.2558
1.0000	0.1261	0.0909	72.0753

FROM SPEC. # 1.00TO SPEC. # 9.00
LEFT SIDE
POSTERIOR
SLICES USED IN AVERAGE= 9.00

XINT	AVG	STDEV	PRCT
0.0000	0.0000	0.0000	0.0000
0.1000	0.1550	0.0449	28.9925
0.2000	0.5111	0.1014	19.8315
0.3000	0.8075	0.0797	9.8729
0.4000	0.9501	0.0318	3.3480
0.5000	0.9969	0.0080	0.7993
0.6000	0.9749	0.0107	1.0930
0.7000	0.8737	0.0394	4.5112
0.8000	0.6857	0.0743	10.8338
0.9000	0.3953	0.1281	32.4160
1.0000	0.0000	0.0000	0.0000

FROM SPEC. # 1.00TO SPEC. # 9.00
RIGHT SIDE
ANTERIOR
SLICES USED IN AVERAGE= 9.00

XINT	AVG	STDEV	PRCT
0.0000	0.9829	0.0135	1.3745
0.1000	0.9965	0.0067	0.6709
0.2000	0.9960	0.0063	0.6323
0.3000	0.9815	0.0104	1.0551
0.4000	0.9478	0.0223	2.3502
0.5000	0.8993	0.0308	3.4277
0.6000	0.8334	0.0405	4.8640
0.7000	0.7617	0.0473	6.2077
0.8000	0.6622	0.0549	8.2846
0.9000	0.4876	0.0604	12.3833
1.0000	0.0197	0.0390	198.4313

FROM SPEC. # 1.00TO SPEC. # 9.00
RIGHT SIDE
POSTERIOR
SLICES USED IN AVERAGE= 9.00

XINT	AVG	STDEV	PRCT
0.0000	0.0000	0.0000	0.0000
0.1000	0.1762	0.0329	18.6670
0.2000	0.5639	0.0852	15.1094
0.3000	0.8254	0.0571	6.9147
0.4000	0.9432	0.0377	3.9973
0.5000	0.9944	0.0079	0.7953
0.6000	0.9741	0.0237	2.4284
0.7000	0.8822	0.0452	5.1272
0.8000	0.7053	0.0654	9.2769
0.9000	0.4261	0.0839	19.9750
1.0000	0.0000	0.0000	0.0000

VERTICALLY DEPENDENT MODEL AT T6 REGION

TABLE 2

FROM SPEC. # 1.00TO SPEC. # 9.00
"LEFT SIDE
ANTERIOR"
SLICES USED IN AVERAGE= 9.00

XINT	AVG	STDEV	PRCT
0.0000	0.9889	0.0171	1.7283
0.1000	0.9838	0.0162	1.6503
0.2000	0.9731	0.0294	3.0163
0.3000	0.9459	0.0426	4.5001
0.4000	0.9040	0.0525	5.8059
0.5000	0.8501	0.0617	7.2605
0.6000	0.7833	0.0682	8.7117
0.7000	0.6973	0.0732	10.4925
0.8000	0.5880	0.0778	13.2390
0.9000	0.4301	0.0768	17.8609
1.0000	0.0359	0.0776	216.1761

FROM SPEC. # 1.00TO SPEC. # 9.00
LEFT SIDE
POSTERIOR
SLICES USED IN AVERAGE= 9.00

XINT	AVG	STDEV	PRCT
0.0000	0.0000	0.0000	0.0000
0.1000	0.1193	0.0583	48.9247
0.2000	0.4589	0.1134	24.7114
0.3000	0.7364	0.0921	12.5004
0.4000	0.9117	0.0599	6.5720
0.5000	0.9803	0.0253	2.5810
0.6000	0.9807	0.0174	1.7715
0.7000	0.9098	0.0496	5.4568
0.8000	0.7938	0.0944	11.8963
0.9000	0.5506	0.1865	34.2365
1.0000	0.0491	0.0986	200.5899

FROM SPEC. # 1.00TO SPEC. # 9.00
RIGHT SIDE
ANTERIOR
SLICES USED IN AVERAGE= 9.00

XINT	AVG	STDEV	PRCT
0.0000	0.9906	0.0139	1.3990
0.1000	0.9839	0.0287	2.9136
0.2000	0.9675	0.0455	4.7067
0.3000	0.9418	0.0561	5.9538
0.4000	0.9055	0.0572	6.3126
0.5000	0.8576	0.0557	6.4908
0.6000	0.7916	0.0583	7.3684
0.7000	0.7123	0.0675	9.4703
0.8000	0.6070	0.0787	12.9706
0.9000	0.4465	0.1068	23.9229
1.0000	0.0847	0.1358	160.4057

FROM SPEC. # 1.00TO SPEC. # 9.00
RIGHT SIDE
POSTERIOR
SLICES USED IN AVERAGE= 9.00

XINT	AVG	STDEV	PRCT
0.0000	0.0000	0.0000	0.0000
0.1000	0.1088	0.0616	56.6709
0.2000	0.4253	0.1213	28.5249
0.3000	0.7334	0.0991	13.5192
0.4000	0.8962	0.0606	6.7657
0.5000	0.9731	0.0276	2.8326
0.6000	0.9772	0.0235	2.4068
0.7000	0.9167	0.0471	5.1415
0.8000	0.7922	0.0756	9.5730
0.9000	0.5146	0.1675	32.5560
1.0000	0.0855	0.1398	163.4582

VERTICALLY DEPENDENT MODEI AT T4 REGION

TABLE 3

COMPARISON OF LEFT AND RIGHT ANTERIOR NORMALIZED DATA

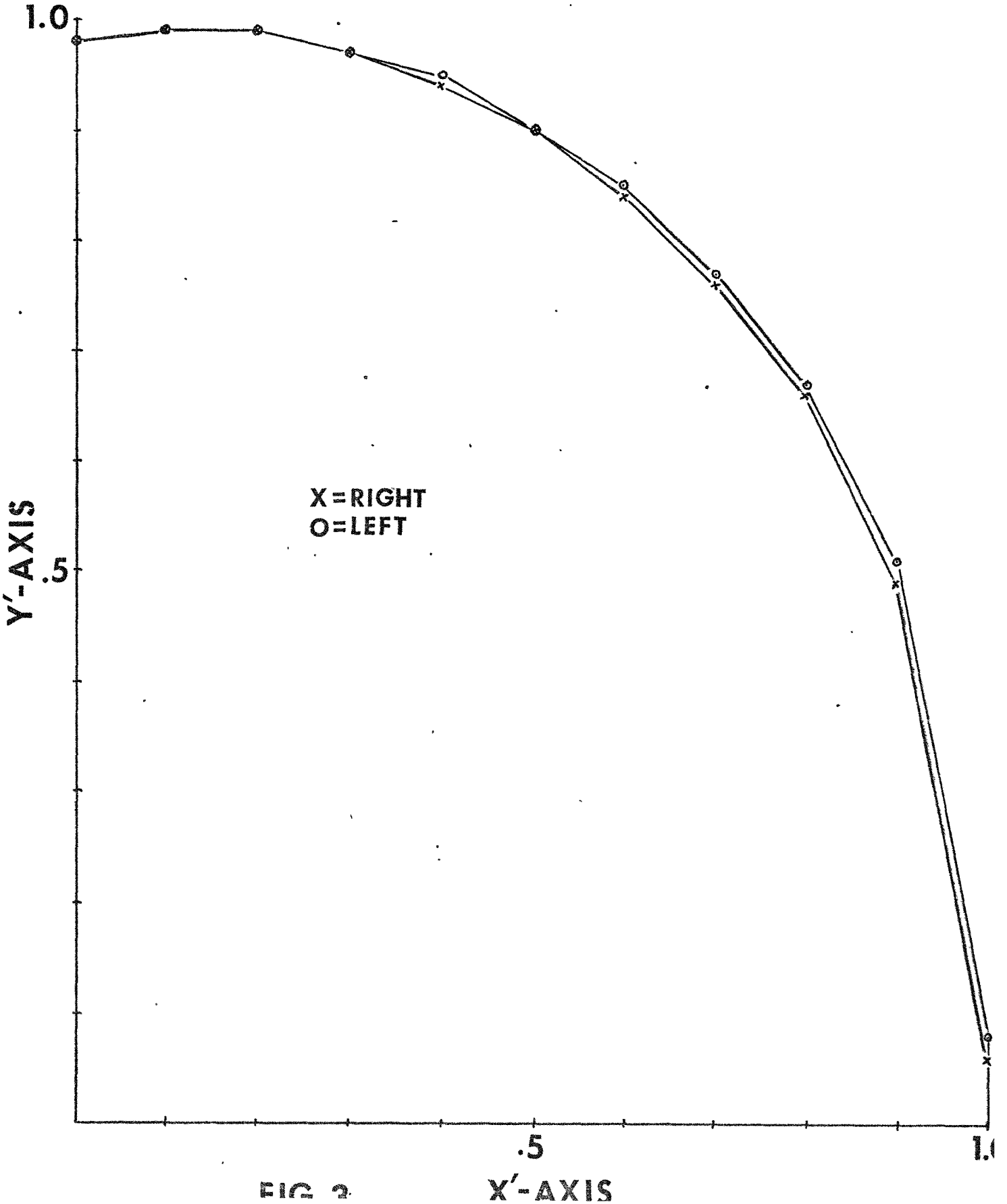

FIG. 3

COMPARISON OF LEFT AND RIGHT POSTERIOR NORMALIZED DATA

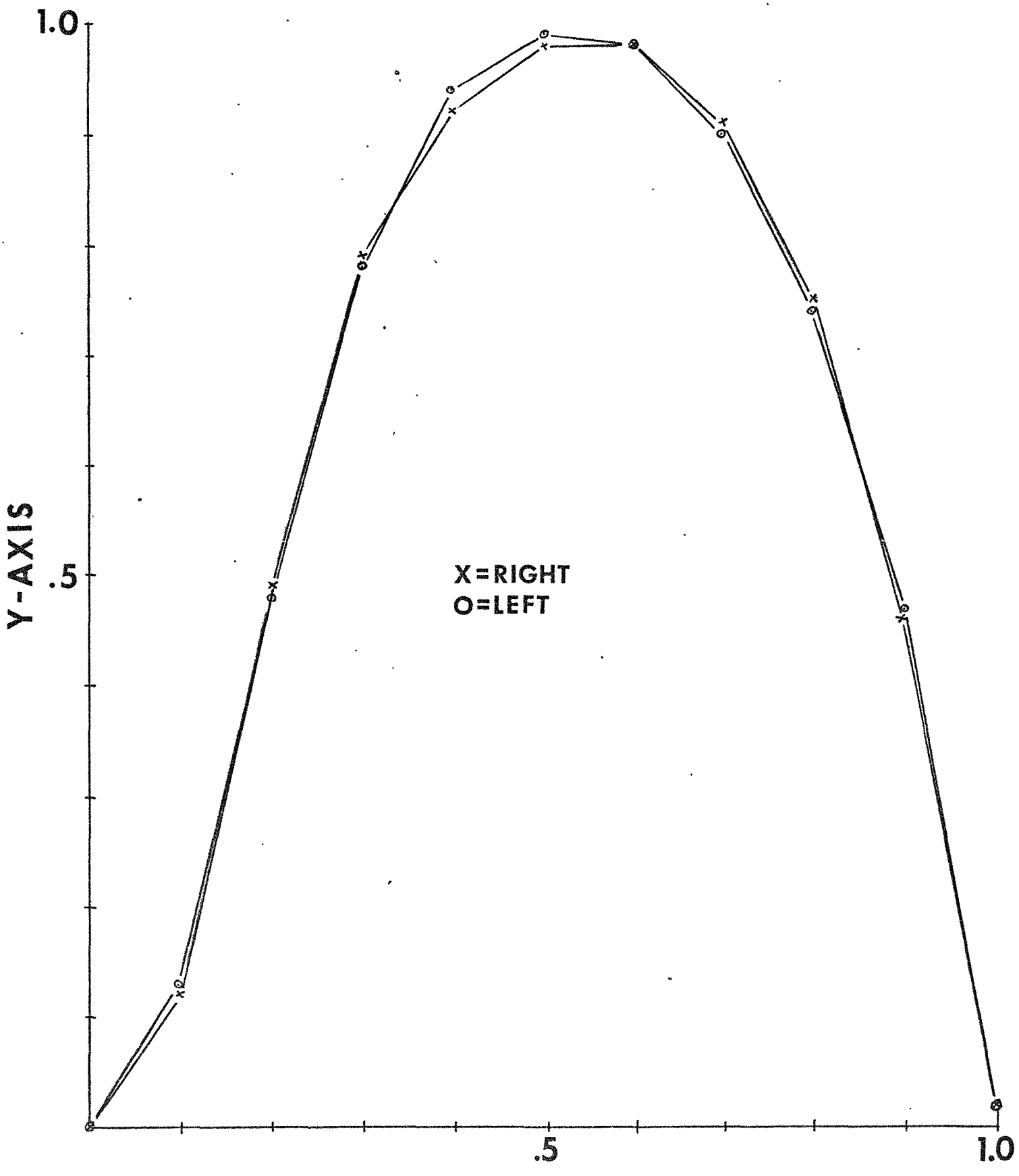

FIG 4

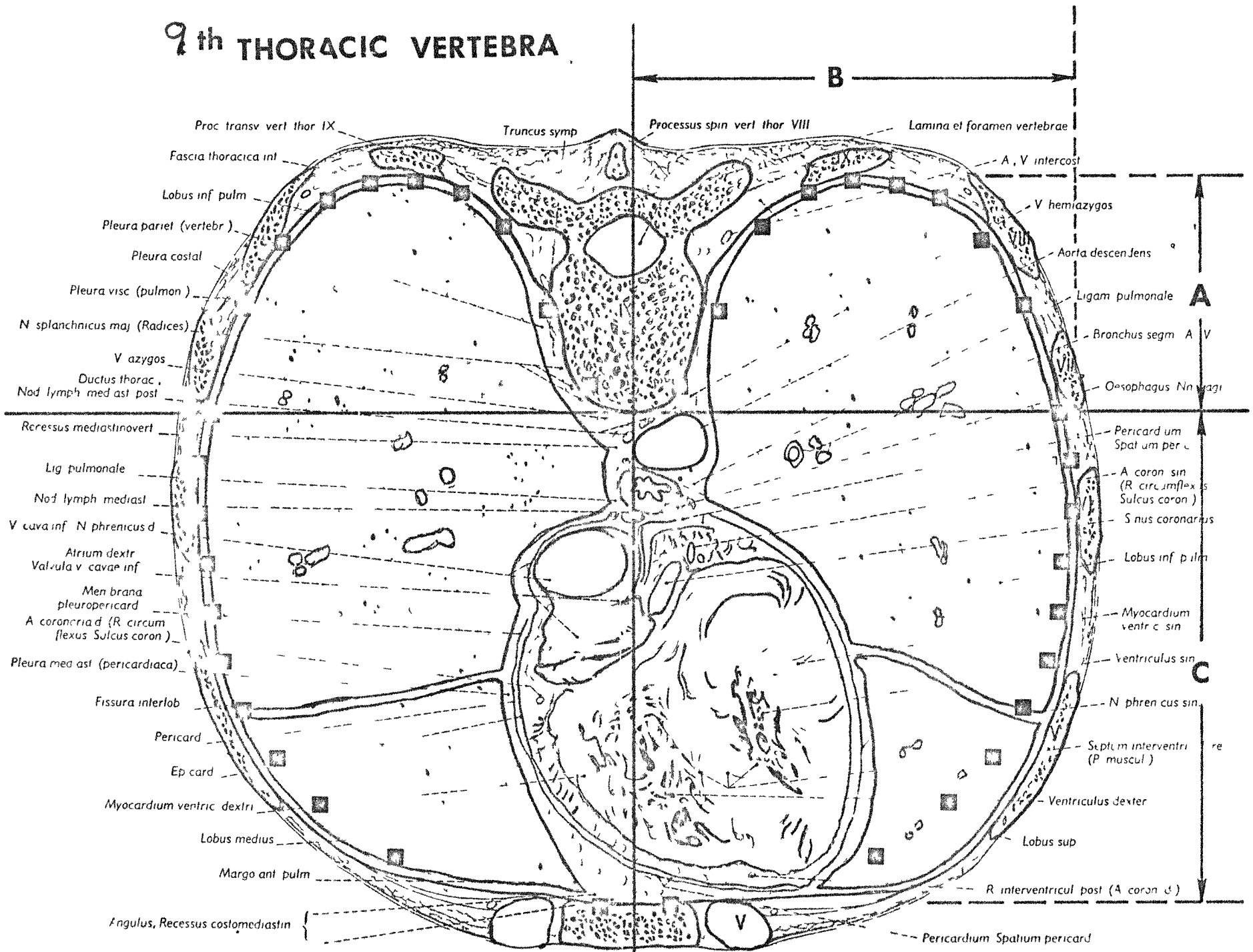
9th THORACIC VERTEBRA
B
A
C
Proc transv vert thor IX
Truncus symp
Processus spin vert thor VIII
Lamina et foramen vertebrae
Fascia thoracica int
A , V intercost
Lobus inf pulm
V hemiazygos
Pleura pariet (vertebr)
Aorta descendens
Pleura costal
Ligam pulmonale
Pleura visc (pulmon)
Bronchus segm A V
N splanchnicus maj (Radices)
V azygos
Ductus thorac ,
Nod lymph med ast post
Oesophagus Nn vagi
Recessus mediastinovert
Pericard um
Spat um per c
Lig pulmonale
A coron sin
(R circumflex is
Sulcus coron)
Nod lymph mediast
S nus coronarius
V cava inf N phrenicus d
Atrium dextr
Valvula v cavae inf
Lobus inf p lm
Men brana
pleuropericard
Myocardium
ventr c sin
A coronaria d (R circum
flexus Sulcus coron)
Ventriculus sin
Pleura med ast (pericardiaca)
N phren cus sin
Fissura interlob
Septum interventri re
(P muscul)
Pericard
Ep card
Ventriculus dexter
Myocardium ventric dextri
Lobus sup
Lobus medius
Margo ant pulm
R interventricul post (A coron d)
Angulus, Recessus costomediastin
V
Pericardium Spatium pericard

FIG. 5

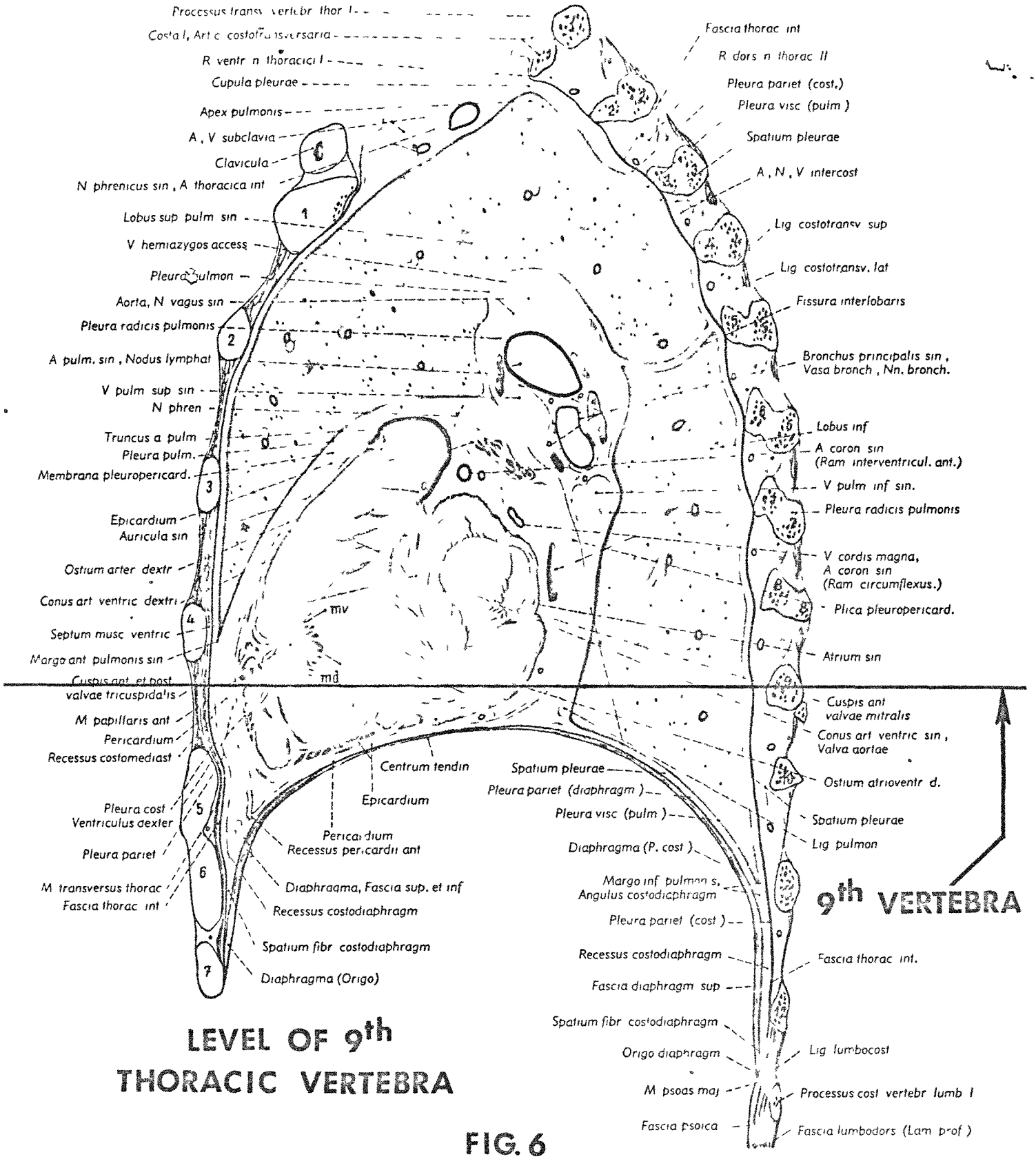
Processus transv vertebr thor I
Costa I, Art c costotransversaria
R ventr n thoracici I
Cupula pleurae
Apex pulmonis
A, V subclavia
Clavicula
N phrenicus sin, A thoracica int
Lobus sup pulm sin
V hemiazygos access
Pleura pulmon
Aorta, N vagus sin
Pleura radicis pulmonis
A pulm. sin, Nodus lymphat
V pulm sup sin
N phren
Truncus a pulm
Pleura pulm.
Membrana pleuropericard.
Epicardium
Auricula sin
Ostium arter dextr
Conus art ventric dextri
Septum musc ventric
Margo ant pulmonis sin
Cuspis ant et post valvae tricuspidalis
M papillaris ant
Pericardium
Recessus costomediast
Pleura cost
Ventriculus dexter
Pleura pariet
M transversus thorac
Fascia thorac int
Centrum tendin
Epicardium
Pericardium
Recessus pericardii ant
Diaphragma, Fascia sup. et inf
Recessus costodiaphragm
Spatium fibr costodiaphragm
Diaphragma (Origo)
mv
md
Fascia thorac int
R dors n thorac II
Pleura pariet (cost.)
Pleura visc (pulm)
Spatium pleurae
A, N, V intercost
Lig costotransv sup
Lig costotransv. lat
Fissura interlobaris
Bronchus principalis sin, Vasa bronch, Nn. bronch.
Lobus inf
A coron sin (Ram interventricul. ant.)
V pulm inf sin.
Pleura radicis pulmonis
V cordis magna, A coron sin (Ram circumflexus.)
Plica pleuropericard.
Atrium sin
Cuspis ant valvae mitralis
Conus art ventric sin, Valva aortae
Ostium atrioventr d.
Spatium pleurae
Lig pulmon
Spatium pleurae
Pleura pariet (diaphragm)
Pleura visc (pulm)
Diaphragma (P. cost)
Margo inf pulmon s, Angulus costodiaphragm
Pleura pariet (cost)
Recessus costodiaphragm
Fascia diaphragm sup
Spatium fibr costodiaphragm
Origo diaphragm
M psoas maj
Fascia psoica
Fascia thorac int.
Lig lumbocost
Processus cost vertebr lumb I
Fascia lumbodors (Lam prof)
9th VERTEBRA
LEVEL OF 9th THORACIC VERTEBRA

FIG. 6

TABLE 4

TRANSFORMATION OF SIMULATED X-RAY MEASUREMENTS FROM FIGURE 5 INTO THE PREDICTED THORAX CAVITY

Simulated X-ray Dimensions: $A' = 4.6$ cm
$B' = 8.6$ cm
$C' = 9.6$ cm

Note: Y_n below is the model for approximately the T9 region

	Left Anterior			Left Posterior		
X_n	$X_n \cdot C'$	Y_n	$Y_n \cdot B'$	$X_n \cdot B'$	Y_n	$Y_n \cdot A'$
0	.0	.971	8.35	0.0	0.0	0.0
.1	.96	.989	8.51	.86	.121	.557
.2	1.92	.996	8.57	1.72	.485	2.23
.3	2.88	.985	8.47	2.58	.803	3.69
.4	3.84	.968	8.32	3.44	.937	4.31
.5	4.8	.941	8.09	4.30	.994	4.57
.6	5.76	.894	7.69	5.16	.983	4.52
.7	6.72	.821	7.06	6.02	.916	4.21
.8	7.68	.716	6.16	6.88	.756	3.48
.9	8.64	.547	4.70	7.74	.458	2.11
1.0	9.6	.083	.71	-	-	-

simulated patient is shown in black squares in Figure 5. Accordingly, to determine a statistical distribution of thorax sizes among the U.S. male population, average values for A, B, and C at each level in the thorax must be determined from a reasonably large sample of x-ray measurements. The procedure used to extract this data from 80 male and 20 female radiograms is described next.

3.1.2 Radiograph Analysis

3.1.2.1 Measurements on Chest Radiographs. One hundred radiographs were read and measured. Eighty of them were chosen from males and twenty from females, since comparison between the male and female chest cavity regarding the shape as well as the size was considered useful. All radiographs were obtained from outpatients of the Cleveland Clinic and were diagnosed "no findings" as far as the thorax was concerned. Their ages ranged between 40 to 55.

Figures 7 and 8 show the front and side view radiographs and the measuring points used. Appendix A gives the details of the measuring method. Approximately 80 measurements are made from each set of radiographs. Some of the data pertains to the location of the outside surface of the heart. The heart dimensions will be examined in detail in the near future but only the chest wall location was analyzed in depth in this reporting period.

Several assumptions were made relative to the radiograph measurements. These assumptions were necessary to solve the problem while not compromising the results.

1. A magnification effect of 10% was assumed at all portions of the radiographs.

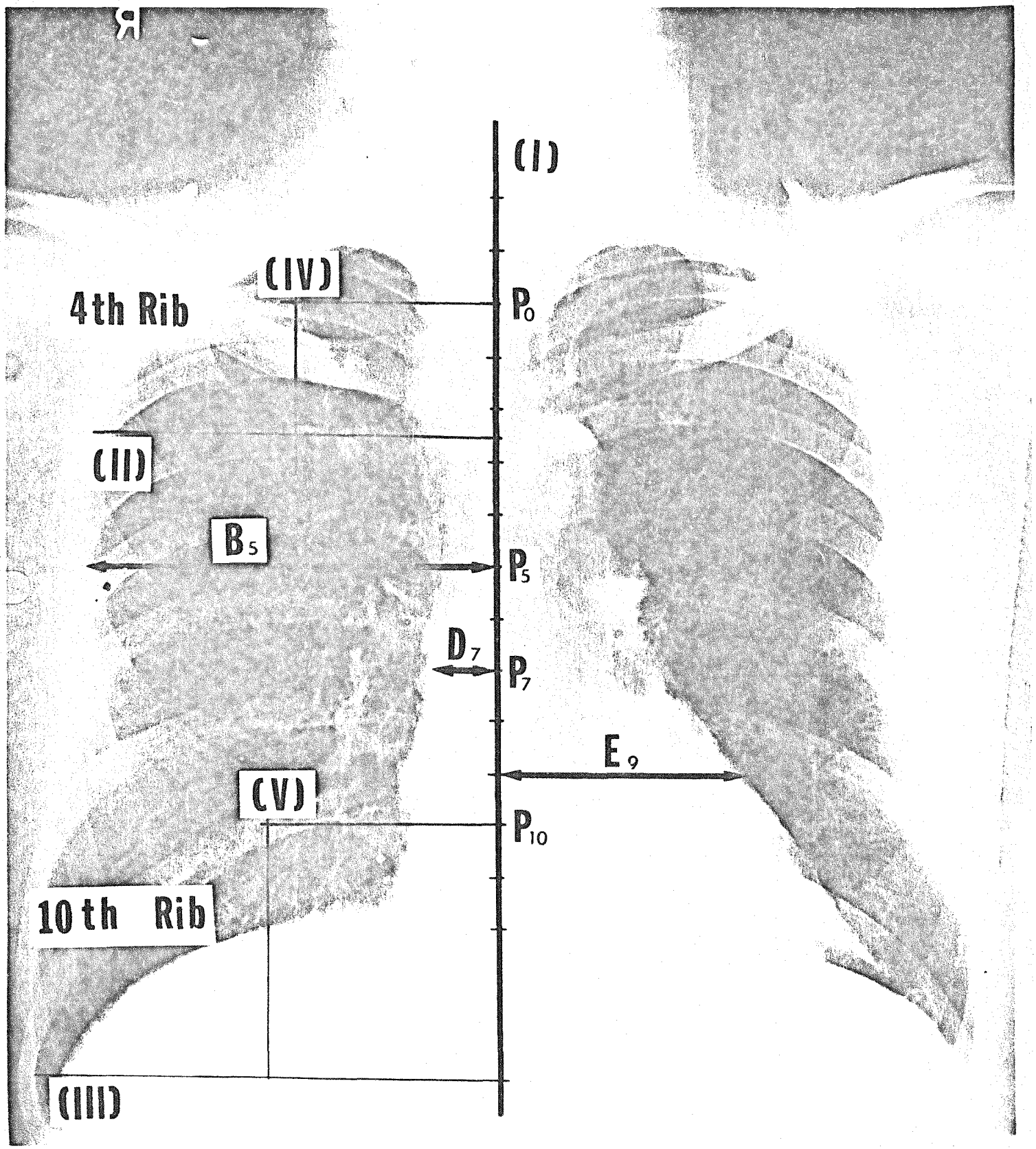

FIGURE 7

FRONT RADIOGRAPH SHOWING DIMENSIONS MEASURED

An average magnification effect is calculated to be 10% by the Department of Radiology at the Cleveland Clinic. Theoretically, it varies according to location on the body relative to the film.

2. The chest cavity is assumed symmetric on a postero-anterior radiograph. The chest is not perfectly symmetric as is usual in other structures of the living body. If all vertebrae clearly appear on a radiograph, a midline can be pointed out without difficulty. Very often, however, some of the thoracic vertebrae, particularly those overlapped with the heart silhouette, are not shown clearly. Thereby, a midline was obtained not anatomically but by dividing the width of the chest cavity by two.

3. All bones are covered with relatively radiotransparent soft tissues. On radiographic measurements, dimensions are obtained as distances between two radioopaque bony structures. However, the mold data yields smaller inside dimensions due to the thickness of these tissues.

4. It was assumed that all patients held a deep inspiration and were standing perpendicular to the floor when the radiographs are made. This is usually the instructions given to the patient. Level of the diaphragmatic dome changes depending upon respiratory phase while configuration of the chest cavity changes depending upon posture. This again accounts for differences between cadavers and living patients.

3.1.2.2 Data Processing. At each level (where a level represents 10% of the distance between the two reference points), the average value, one standard deviation, and the percent that this standard deviation is of the average was calculated. Tables 5 and 6 summarize this data for

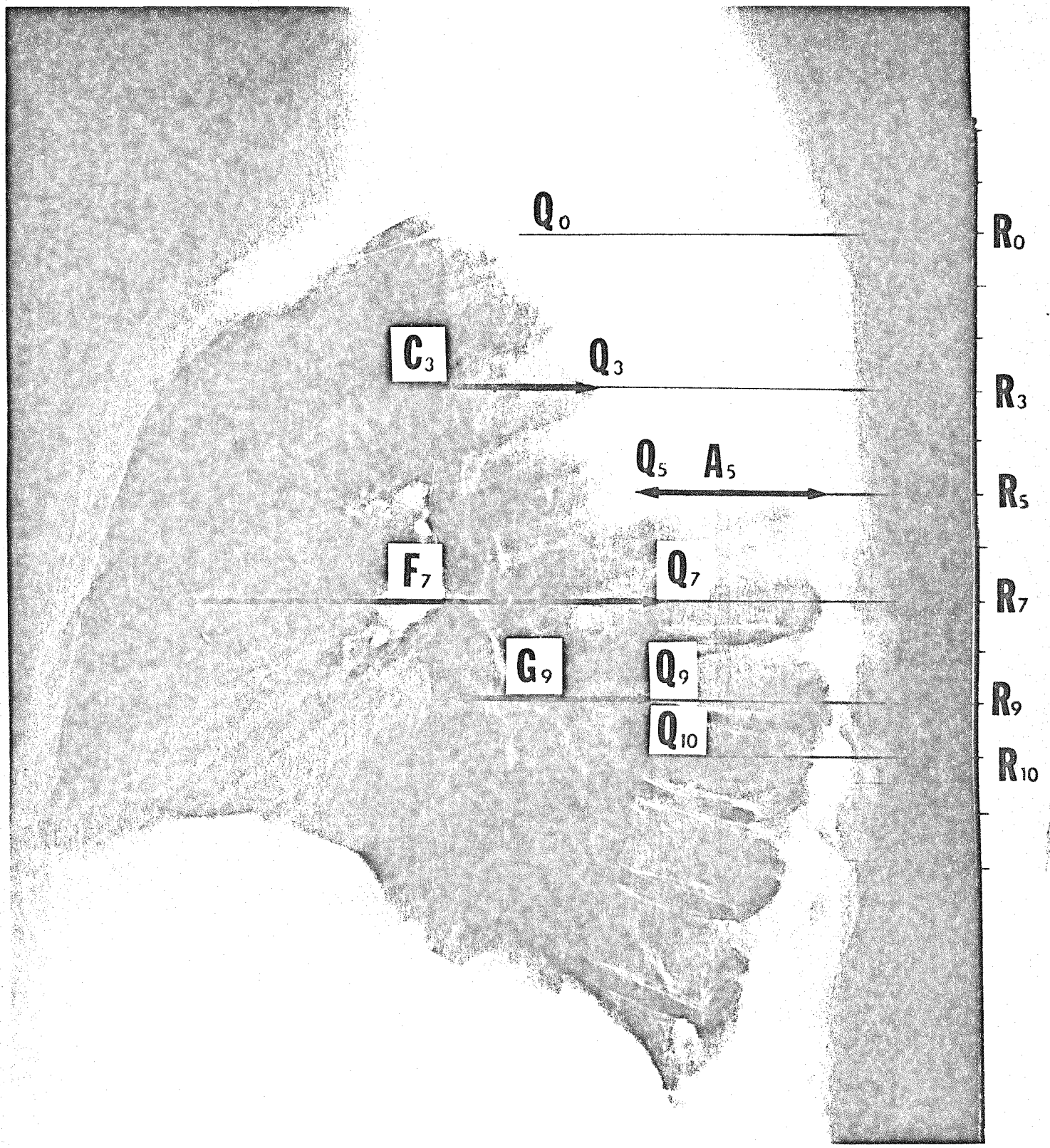

FIGURE 8

SIDE RADIOGRAPH SHOWING DIMENSIONS MEASURED

TABLE 5

SUMMARY OF MALE X-RAY DATA

Level	Normalizing Parameter: B			C			A		
	Avg.	σ	$\frac{\sigma}{\text{Avg.}} \times 100$	Avg.	σ	$\frac{\sigma}{\text{Avg.}} \times 100$	Avg.	σ	$\frac{\sigma}{\text{Avg.}} \times 100$
-2	4.74	0.69	14.7	1.03	0.68	66.5	1.80	0.00	0.0
-1	7.14	1.42	19.9	4.91	2.62	53.4	3.36	1.39	41.5
0 Ref	9.18	1.02	11.1	7.84	2.11	26.9	4.70	0.79	16.9
1	10.52	0.88	8.3	9.79	1.81	18.5	4.97	0.72	14.4
2	11.26	0.84	7.5	10.97	1.61	14.7	5.15	0.64	12.3
3	11.70	0.80	6.8	11.84	1.62	13.7	5.28	0.60	11.3
4	12.13	0.77	6.3	12.47	1.74	13.9	5.41	0.59	11.0
5	12.38	0.78	6.3	12.87	1.83	14.2	5.53	0.61	11.1
6	12.63	0.83	6.6	13.13	1.91	14.6	5.65	0.63	11.1
7	12.86	0.83	6.5	13.23	2.02	15.3	5.77	0.63	11.0
8	13.08	0.89	6.8	13.22	2.11	15.9	5.89	0.65	11.0
9	13.23	1.04	7.9	13.07	2.13	16.3	5.99	0.68	11.4
10 Ref	13.65	0.95	7.0	12.85	1.98	15.4	6.04	0.70	11.5
11	13.91	0.83	6.0	12.48	1.99	16.0	6.12	0.69	1.3
12	14.05	.87	6.2	12.12	1.90	15.7	6.19	0.79	12.8

TABLE 6

SUMMARY OF FEMALE X-RAY DATA

Level	Normalizing Parameter B			C			A		
	Avg.	σ	$\frac{\sigma}{\text{Avg.}} \times 100$	Avg.	σ	$\frac{\sigma}{\text{Avg.}} \times 100$	Avg.	σ	$\frac{\sigma}{\text{Avg.}} \times 100$
-2	3.92	0.45	11.4	0.45	0.00	0.0			
-1	6.50	1.62	15.7	2.97	1.74	58.4	1.79	0.66	36.7
0 Ref	8.52	0.83	9.7	6.32	1.80	28.4	3.31	0.48	14.6
1	9.71	0.73	7.5	8.51	1.28	15.0	3.78	0.40	10.6
2	10.33	0.73	7.0	9.63	1.33	13.8	4.12	0.44	10.7
3	10.61	0.73	6.9	10.31	1.50	14.6	4.37	0.45	10.4
4	11.00	0.75	6.9	10.91	1.48	13.5	4.58	0.46	10.0
5	11.12	0.75	6.8	11.11	1.52	13.7	4.76	0.49	10.3
6	11.22	0.79	7.1	11.13	1.44	12.9	5.00	0.51	10.3
7	11.34	0.82	7.2	11.07	1.51	13.6	5.18	0.59	11.3
8	11.45	0.89	7.7	10.86	1.53	14.1	5.28	0.64	12.1
9	11.51	0.87	7.6	10.71	1.64	15.4	5.36	0.61	11.5
10 Ref	11.58	0.87	7.5	10.16	1.65	16.2	5.42	0.62	11.4
11	11.76	1.08	9.2	9.52	0.97	10.2	5.36	0.66	12.3
12	12.13	0.70	5.8	8.69	0.28	3.2	5.57	0.59	10.6

males and females, respectively. Distance between the two reference points for males was 16.57 ± 1.31 cm and 15.77 ± .73 for females.

Comparison of X-Ray and Mold Data. To check the assumption of dimensional symmetry in the thorax, as opposed to the symmetry of "shape" described earlier, left and right measurements for the normalizing parameters A and B were taken from the mold data and plotted against each other in Figures 9 and 10. Regression lines (solid) were calculated and are shown compared with the dotted identity line. Slopes of these regressions were .92 for A (y intercept = .51) and .83 for B (y intercept = 1.85). Perfect symmetry would have resulted in a slope of 1 and y intercept values of 0. This minor lack of symmetry, however, besides being within the expected error in the process of generating molds (they are used primarily for "shape" information rather than absolute measurements), would result in a negligible error in the overall predicted distributions.

Besides the dimensional symmetry check on the raw mold data, comparisons were made between x-ray and mold data at various vertical levels in the chest. Summarized in Figures 11 through 13 are plots of the male x-ray data showing the average dimension (± two standard deviations) at various vertical levels in the chest. This is just a graphical representation of the data in Tables 5 and 6, and is used as a framework for comparing the x-ray data with the mold data. The mold measurements should be approximately from the same statistical distribution as the x-ray data. Parameter A, shown in Figures 14 and 15 showed the best correlation although the mold dimensions were slightly less than the radiogram distribution. This discrepancy probably reflects the fact that soft tissue

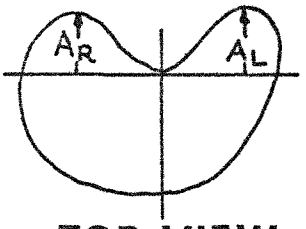

COMPARISON OF NORMALIZING PARAMETERS (A_R vs. A_L) FROM MOLD DATA

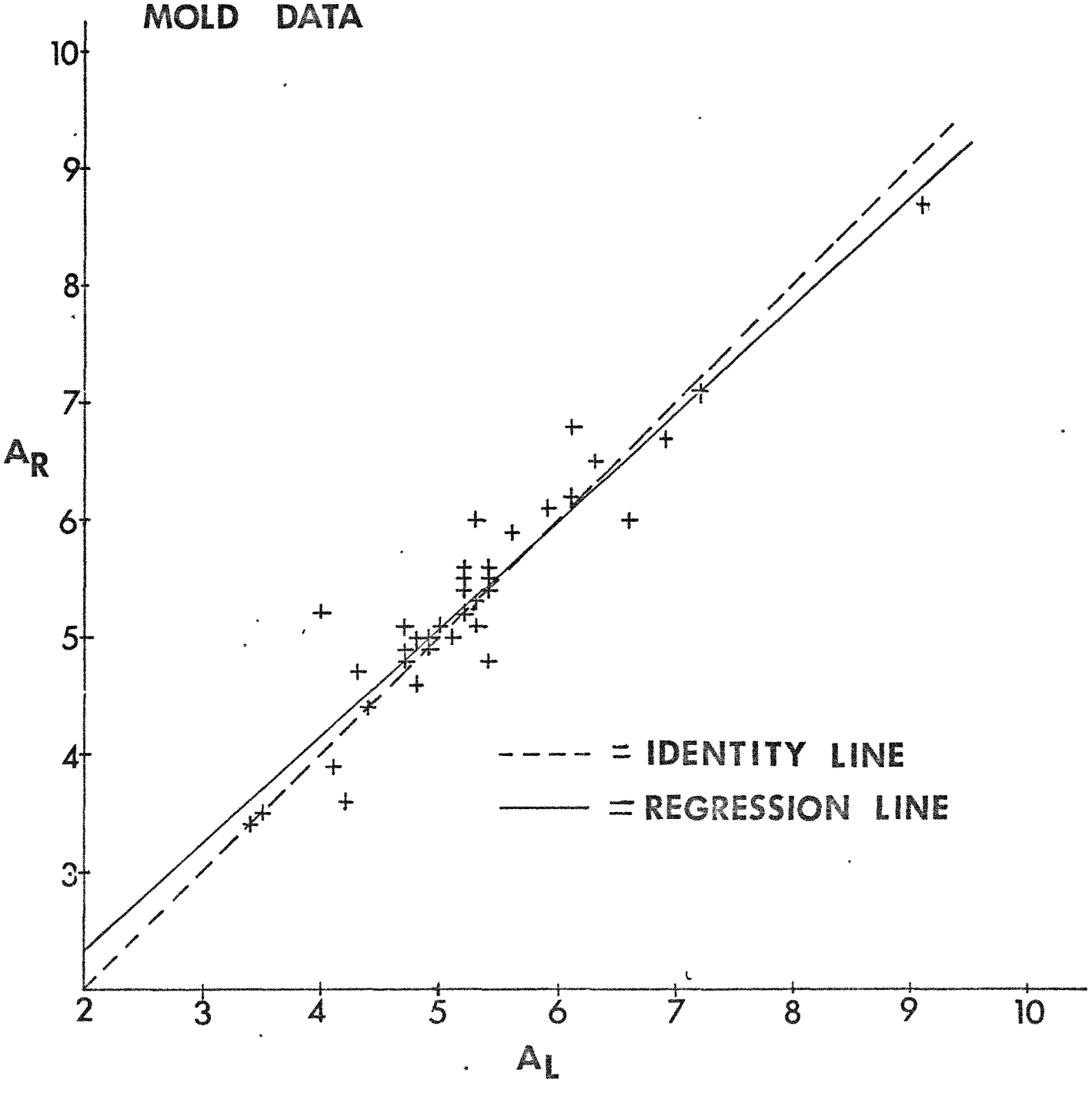

FIG. 9

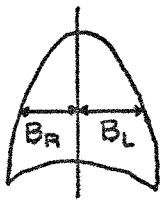

FRONT VIEW

COMPARISON OF NORMALIZING PARAMETERS (B_R vs. B_L) FROM MOLD DATA

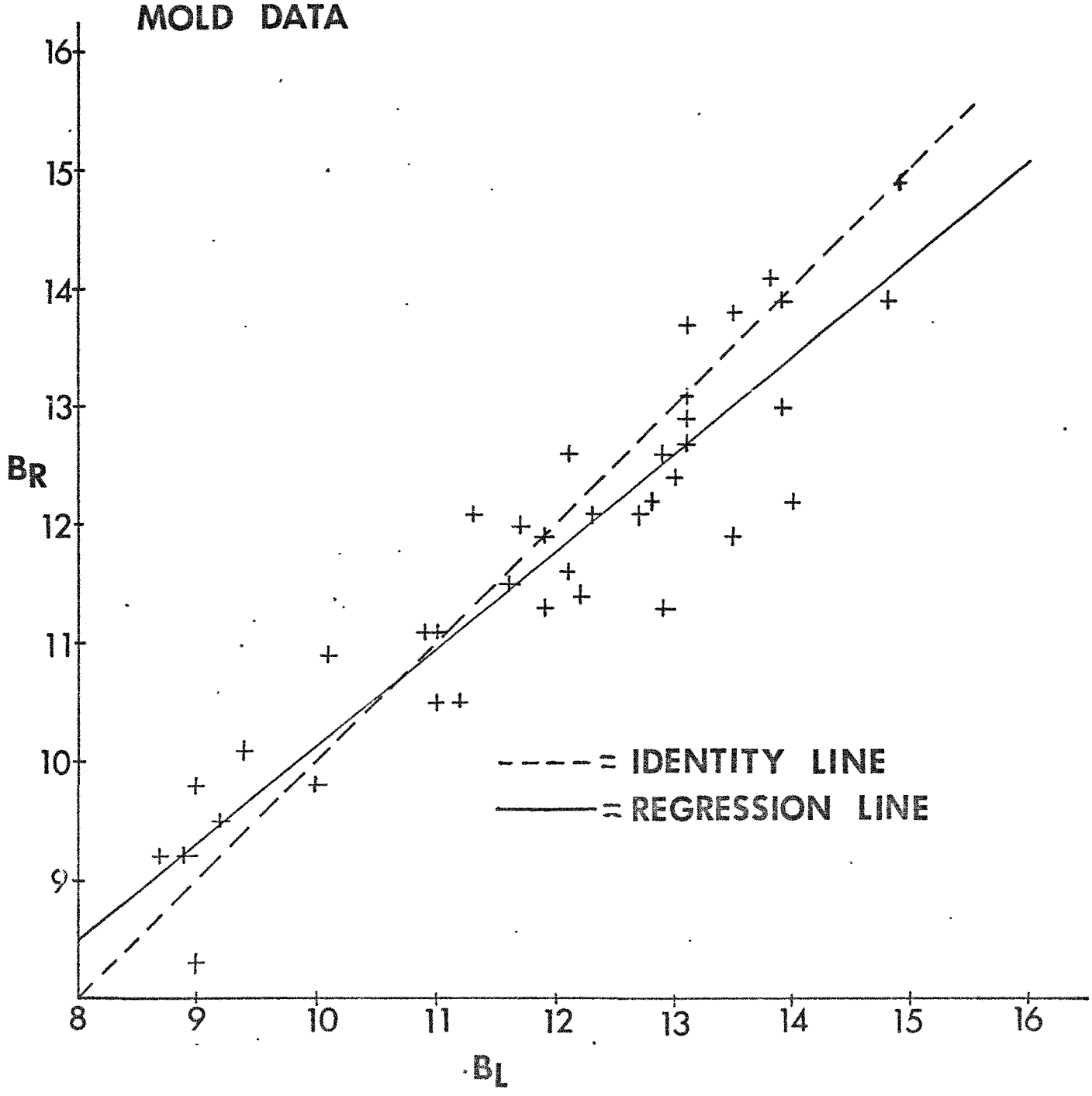

FIG. 10

MALE X-RAY DATA

DORSAL DIMENSION (A), SIDE VIEW

AVG. ± 2 ST. DEV.

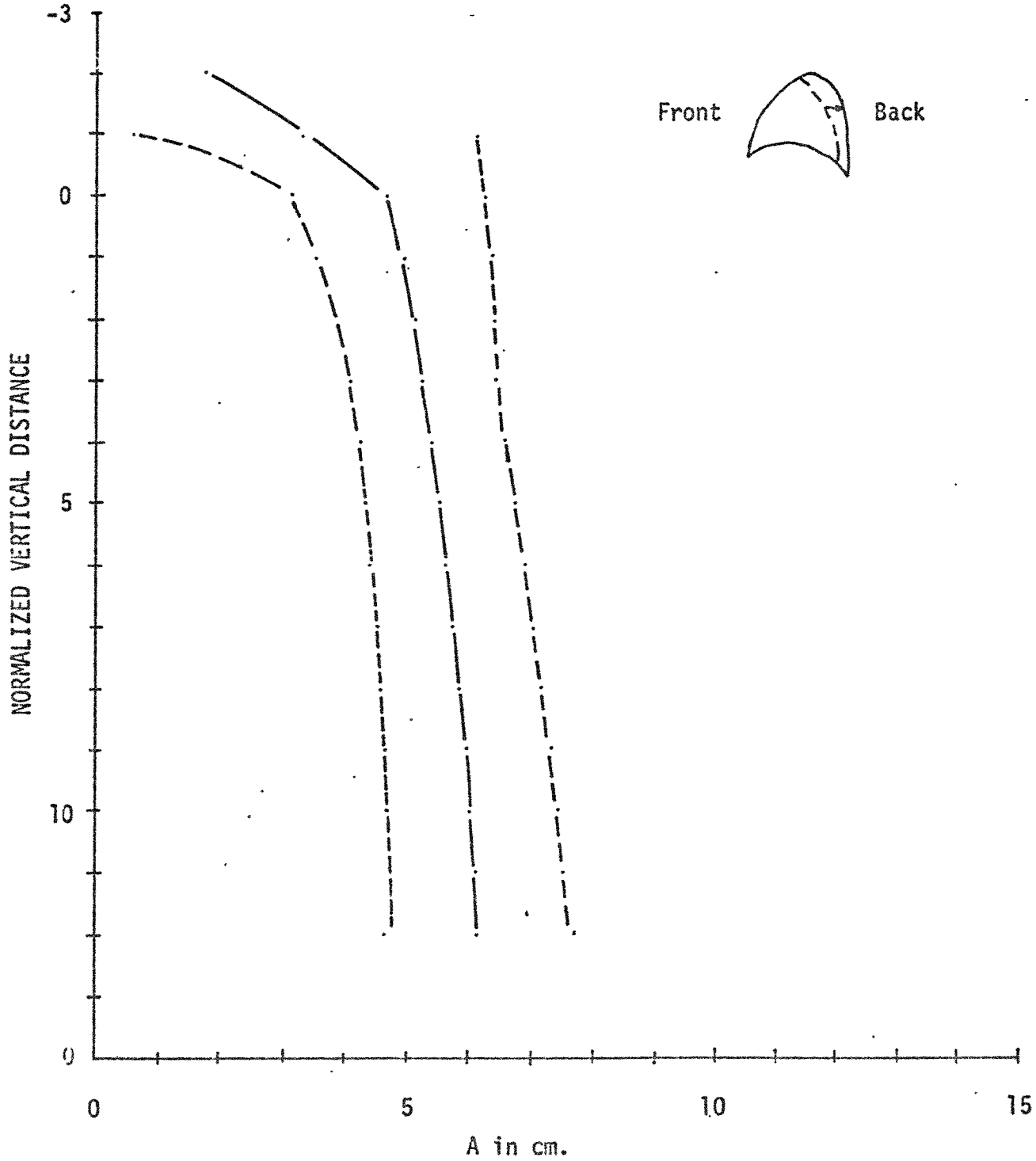

FIGURE 11

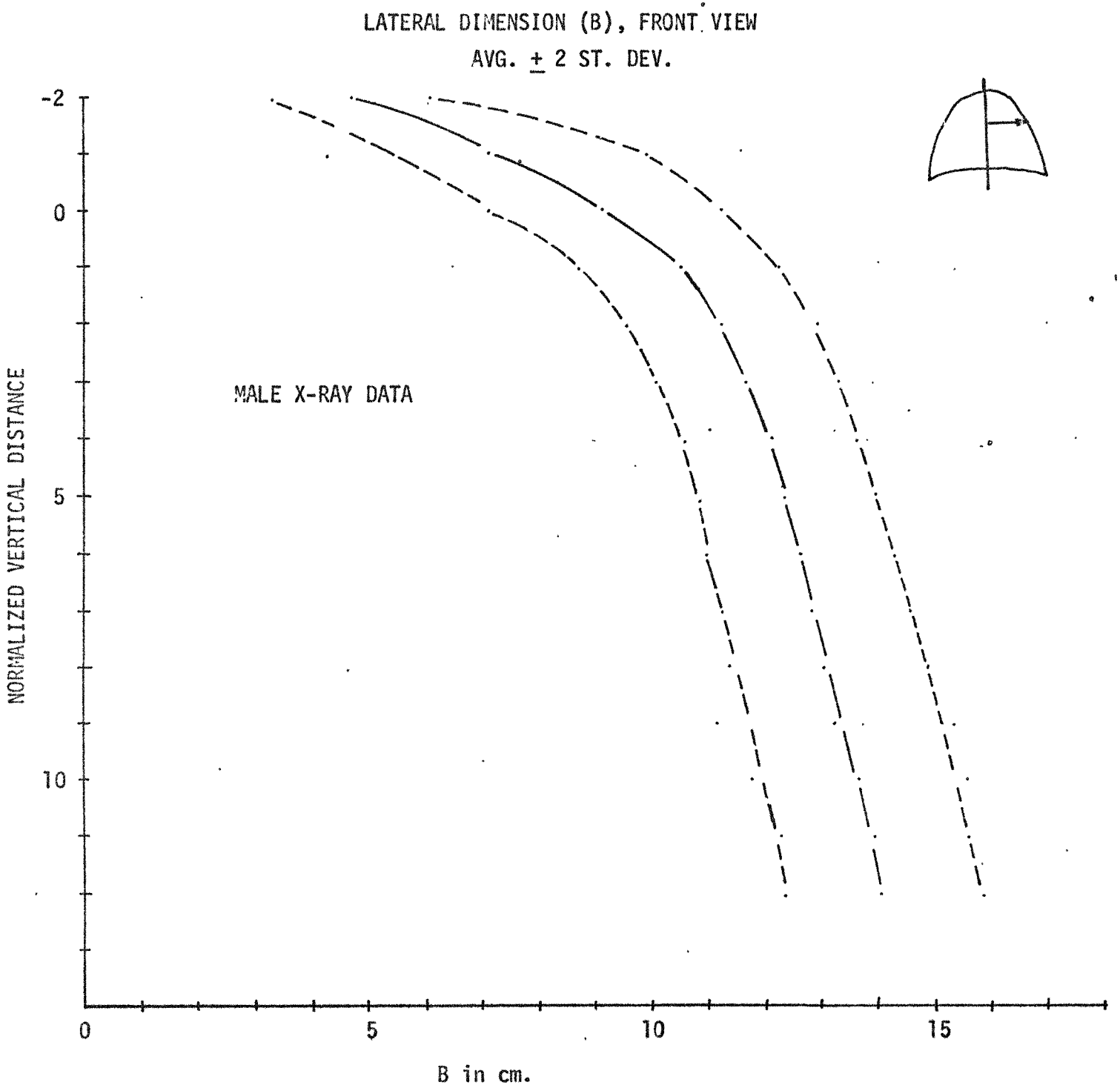
LATERAL DIMENSION (B), FRONT VIEW
AVG. ± 2 ST. DEV.
MALE X-RAY DATA
NORMALIZED VERTICAL DISTANCE
-2
0
5
10
0
5
10
15
B in cm.

FIGURE 12

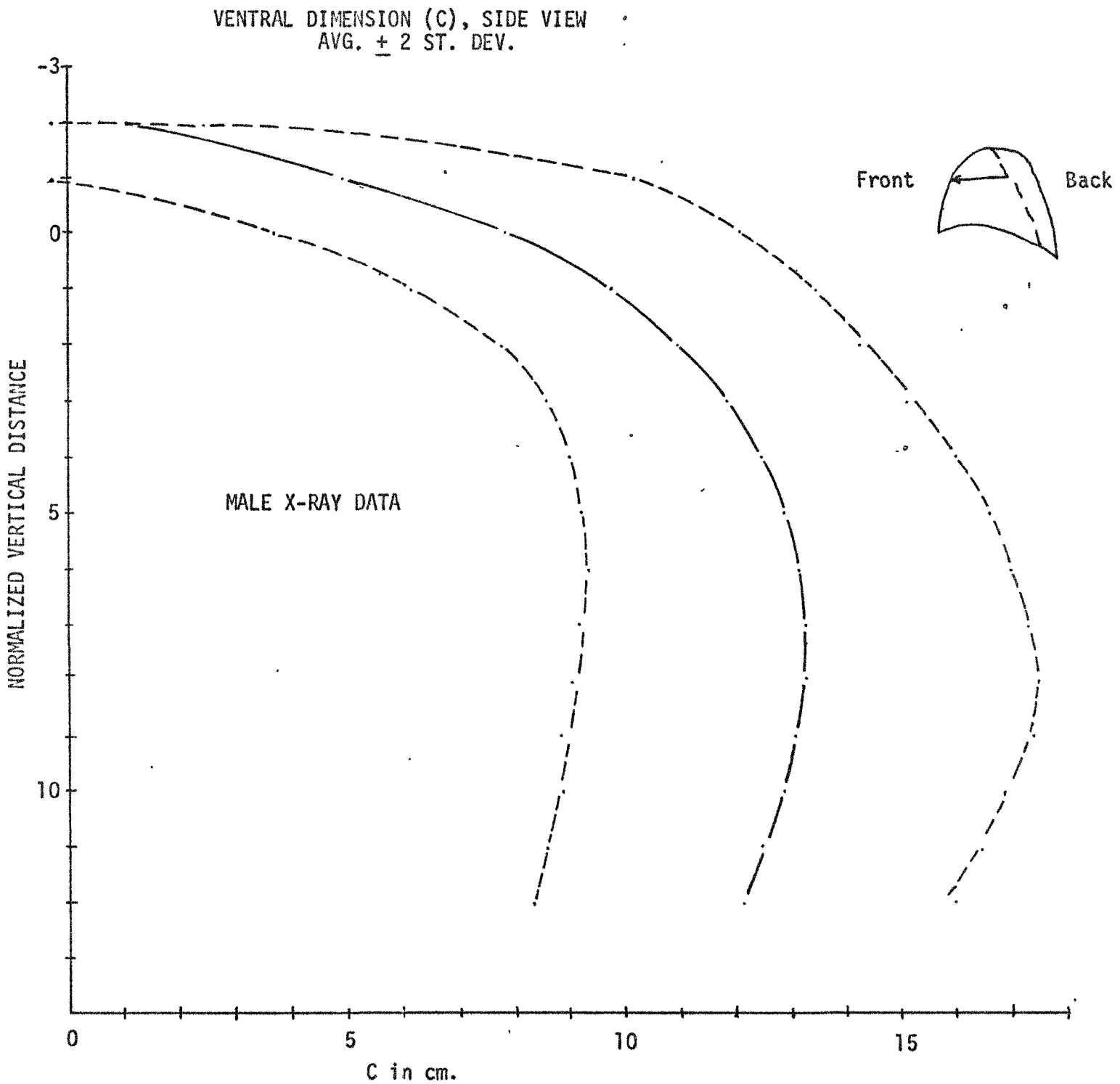
VENTRAL DIMENSION (C), SIDE VIEW
AVG. ± 2 ST. DEV.
-3
0
5
10
NORMALIZED VERTICAL DISTANCE
MALE X-RAY DATA
Front
Back
0
5
10
15
C in cm.

FIGURE 13

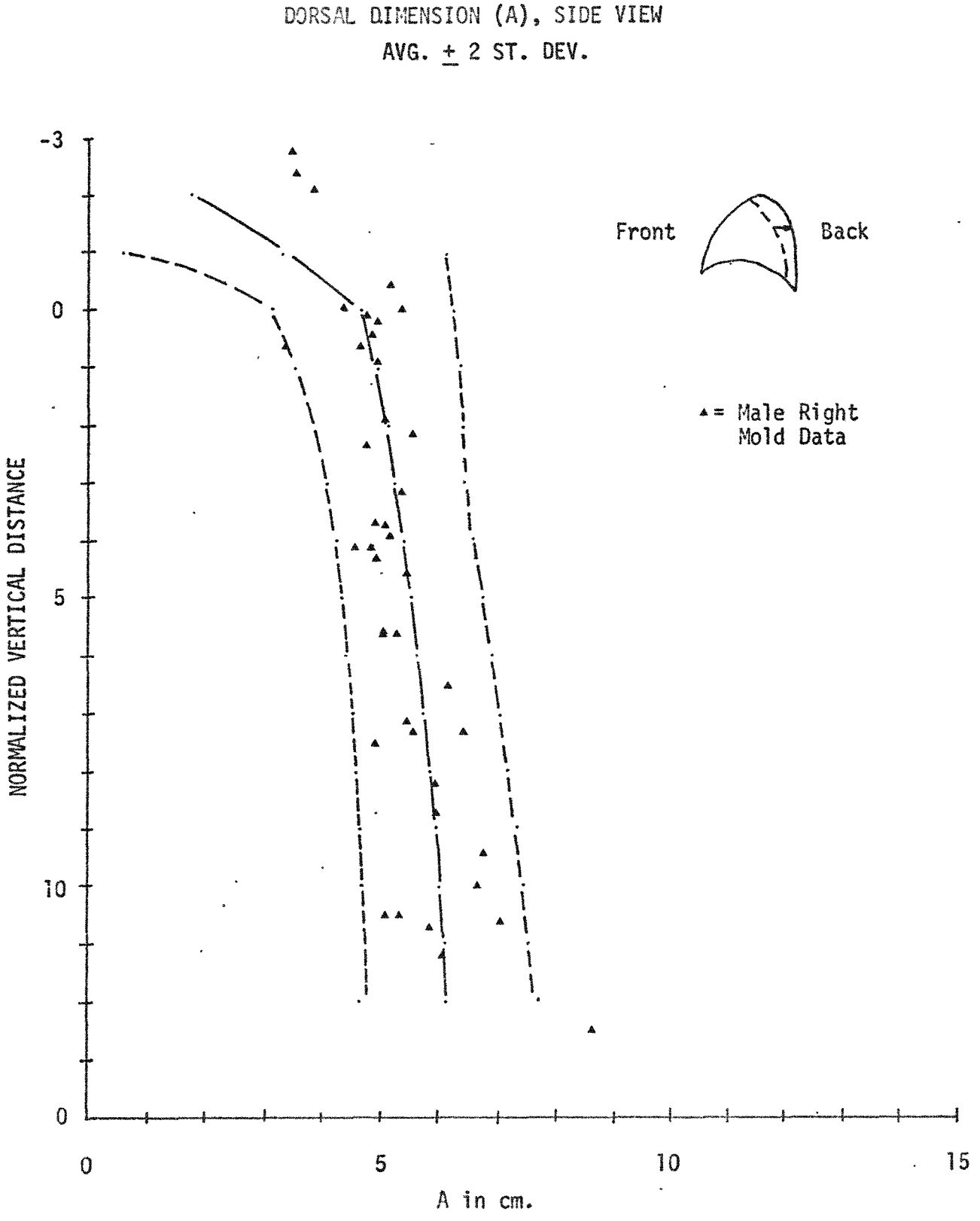
DORSAL DIMENSION (A), SIDE VIEW
AVG. ± 2 ST. DEV.
-3
0
5
10
0
5
10
15
NORMALIZED VERTICAL DISTANCE
A in cm.
Front
Back
▲= Male Right
Mold Data

FIGURE 14

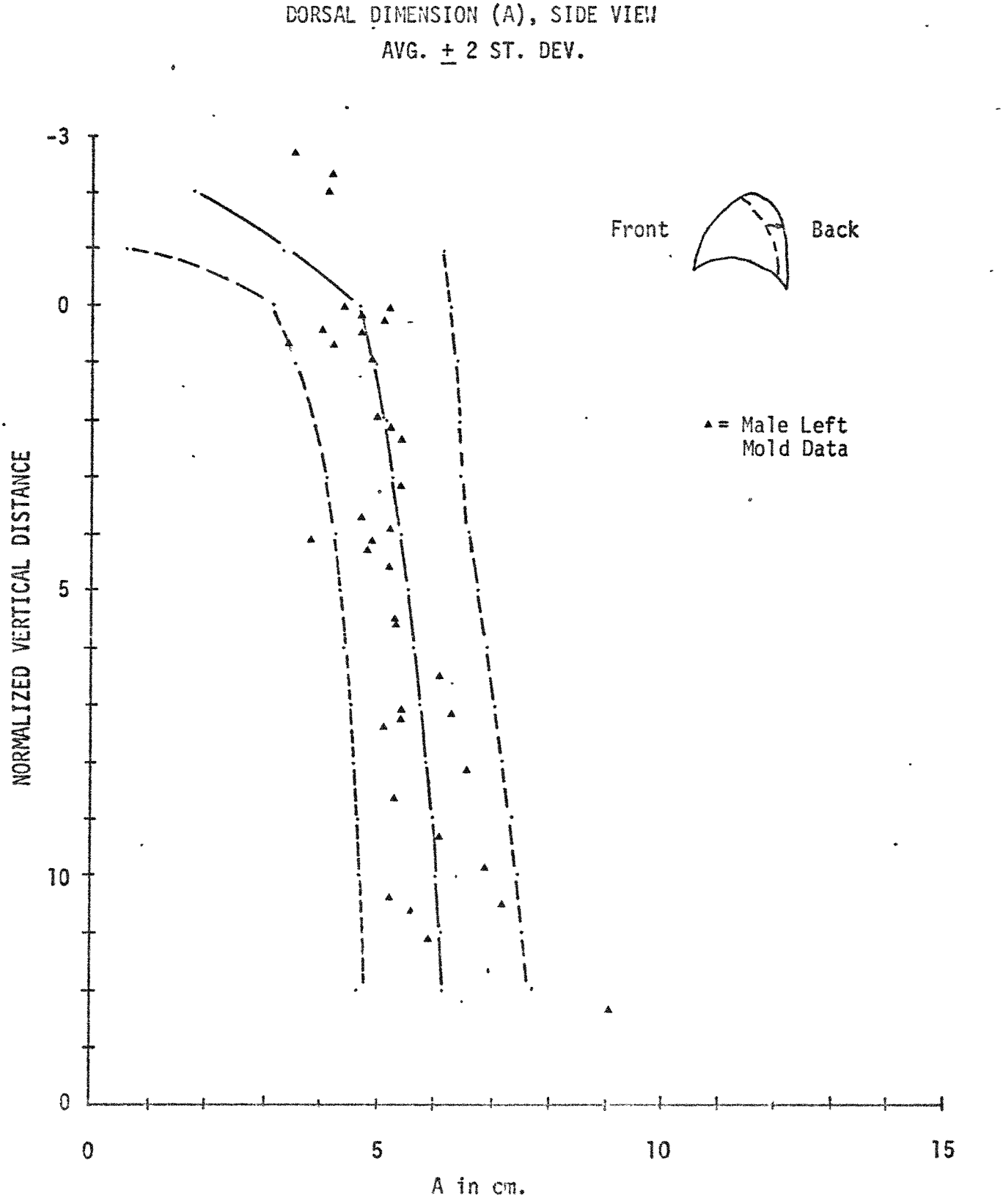
DORSAL DIMENSION (A), SIDE VIEW
AVG. ± 2 ST. DEV.
NORMALIZED VERTICAL DISTANCE
-3
0
5
10
0
5
10
15
A in cm.
Front
Back
▲= Male Left
Mold Data

FIGURE 15

between the actual chest cavity and the rib cage does not show up on x-ray film. Mold data in Figures 16 and 17, for parameter B, was also fairly close to the radiogram data. Parameter C, shown in Figure 18, showed the largest difference (again the mold data smaller than x-ray data). The difference could be due to the fact that x-rays are taken during inspiration, while cadavers represent practically full expiration. Considering the "pump handle" action of the ribs during respiration, the somewhat larger difference is not surprising. Figures 19 through 21 demonstrate the quite marked difference between male and female chest dimensions. The smaller size, especially in the heart region could be a limiting factor in the design of a universal cardiac prosthesis.

3.1.3 Integration of Model and Radiograms

Applying the vertically dependent model (summarized in Tables 1 through 3) to the x-ray data, results in the desired statistical chest size distributions shown in Figures 22 through 24. These figures are actual size and represent the average x-ray parameters (plus and minus two standard deviations) for the upper, middle, and lower thorax regions. Hence, the inner and outer two dotted lines include 95% of the male adult population. Also shown, in numerical figures, are the percent values for that portion of the population smaller than the indicated curve. Hopefully, meaningful external design constraints for an artificial heart can be determined when these curves are combined with the relative location of vital soft structures.

Conclusions. A preliminary vertically dependent model for generating thorax curvature from two dimensional radiograms has been combined with

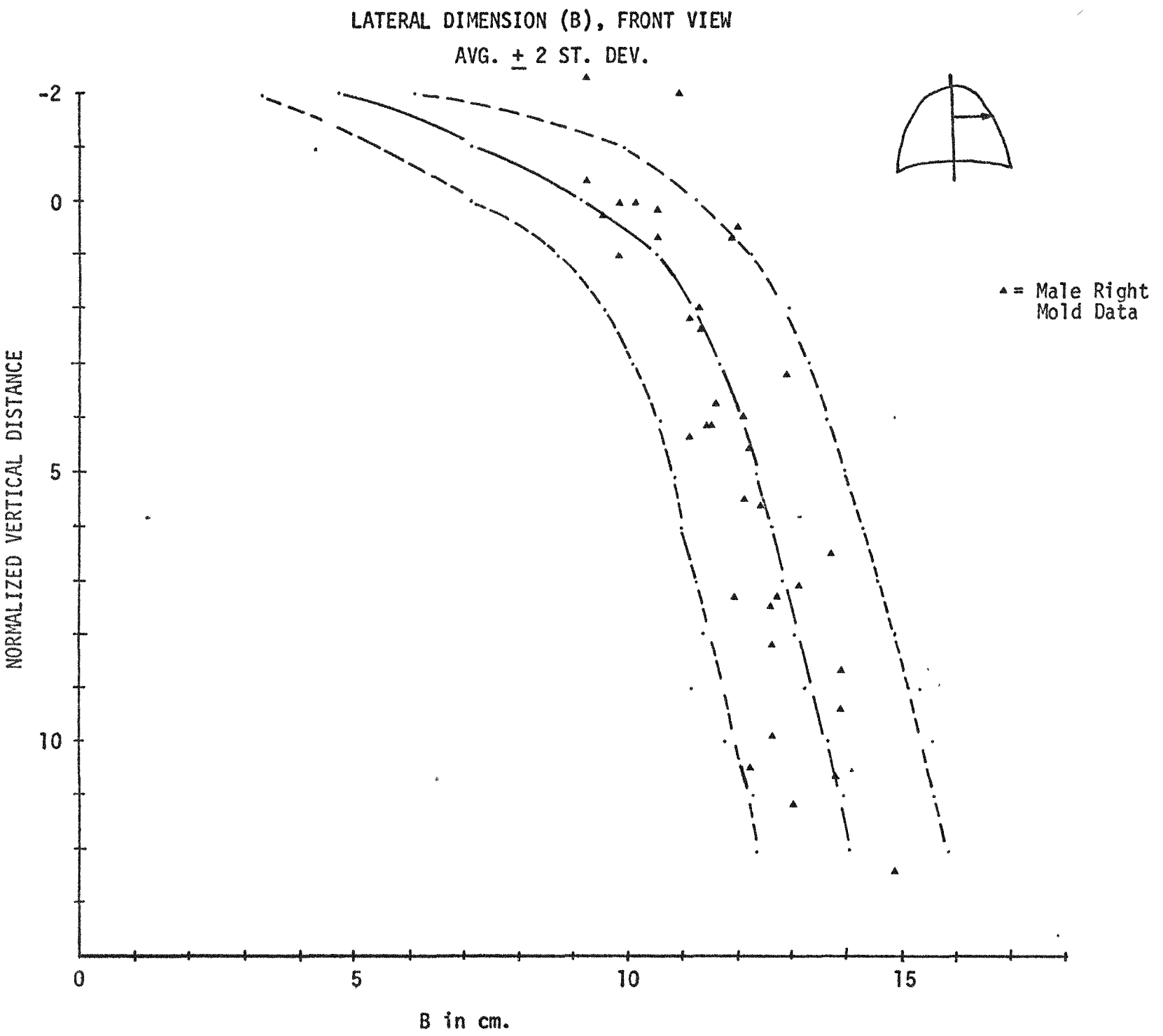
LATERAL DIMENSION (B), FRONT VIEW
AVG. ± 2 ST. DEV.
NORMALIZED VERTICAL DISTANCE
-2
0
5
10
0
5
10
15
B in cm.
▲ = Male Right Mold Data

FIGURE 16

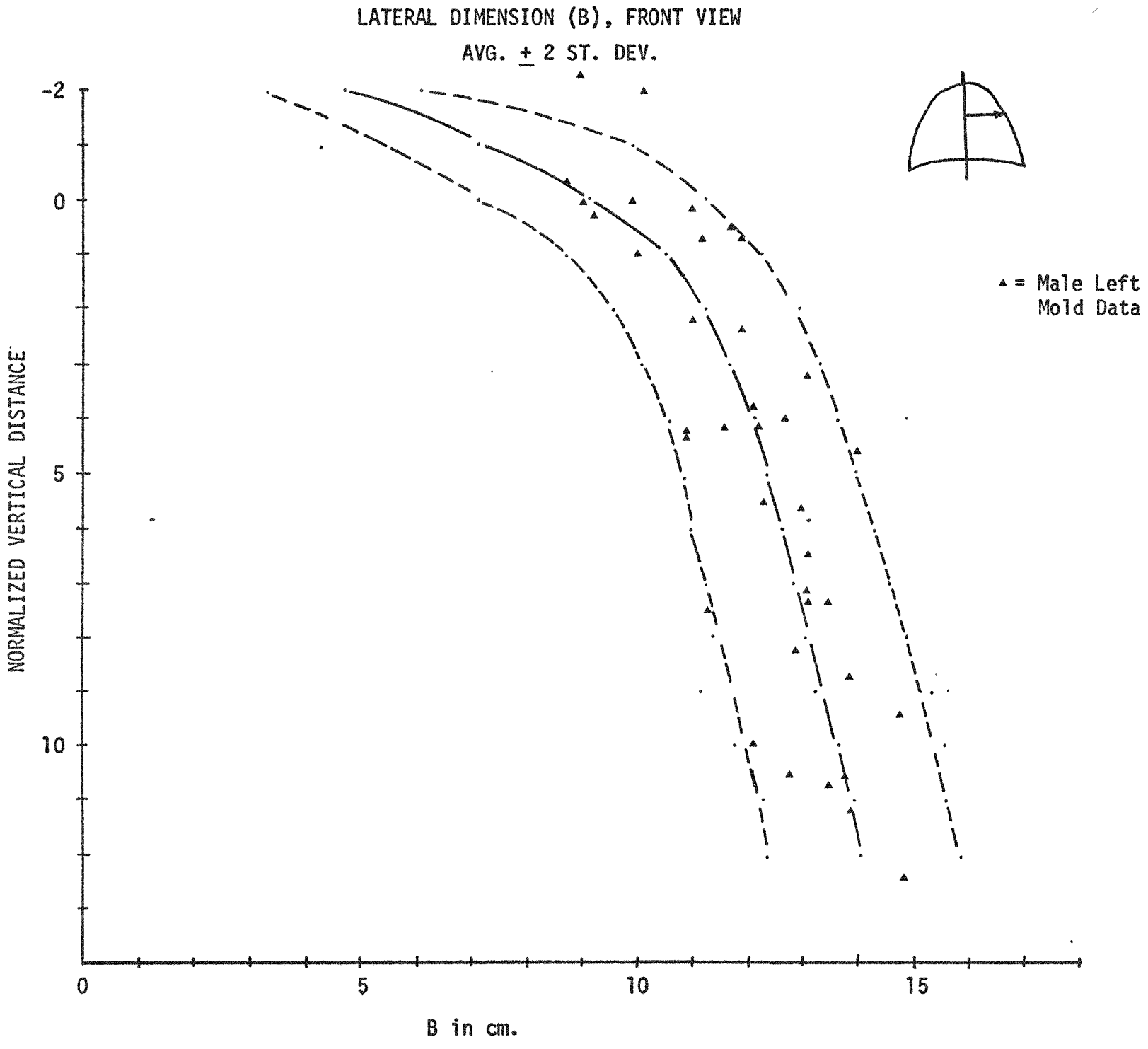
LATERAL DIMENSION (B), FRONT VIEW
AVG. ± 2 ST. DEV.
-2
0
5
10
NORMALIZED VERTICAL DISTANCE
0
5
10
15
B in cm.
▲ = Male Left
Mold Data

FIGURE 17

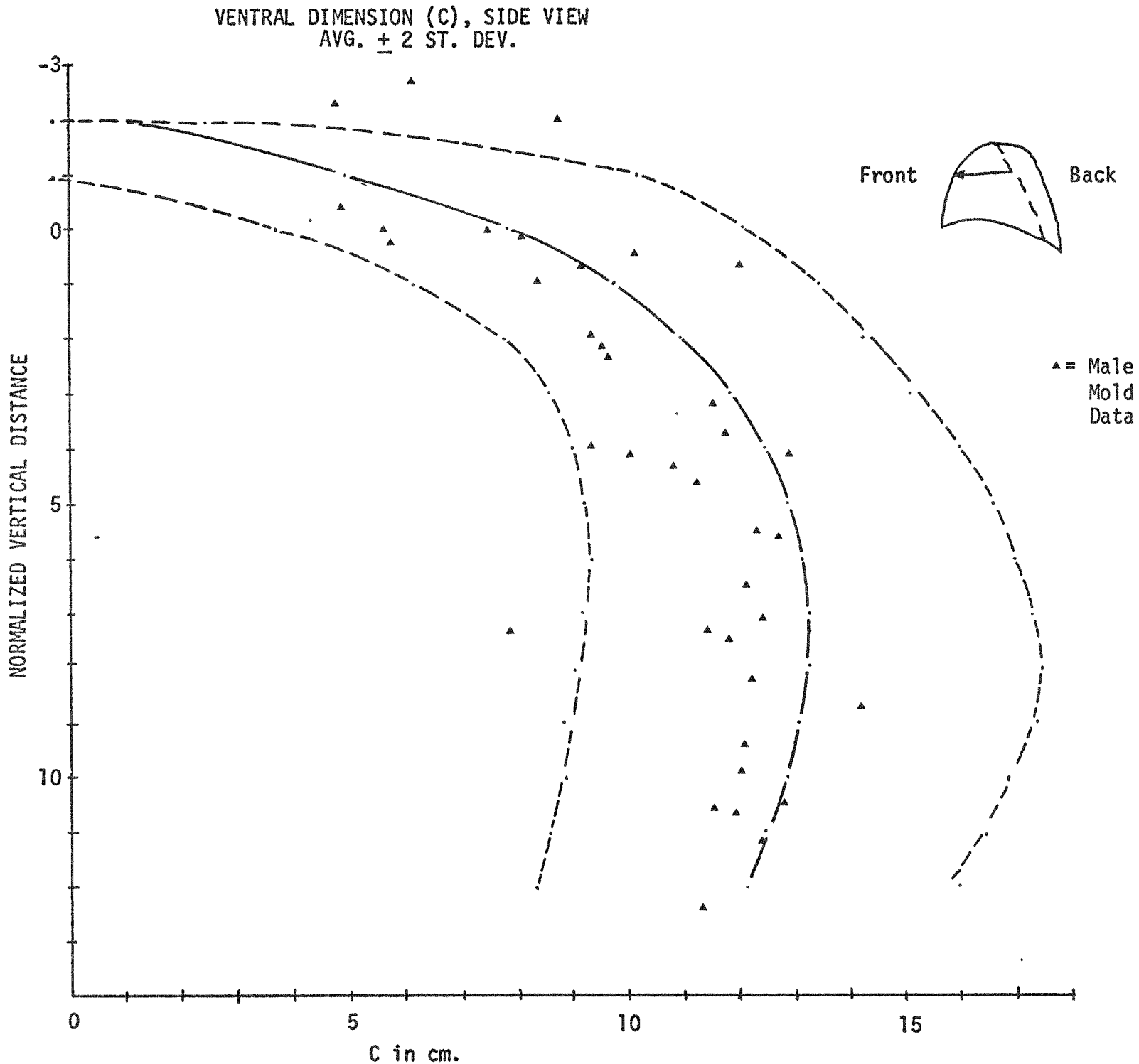
VENTRAL DIMENSION (C), SIDE VIEW
AVG. ± 2 ST. DEV.
NORMALIZED VERTICAL DISTANCE
-3
0
5
10
0
5
10
15
C in cm.
Front
Back
▲= Male
Mold
Data

FIGURE 18

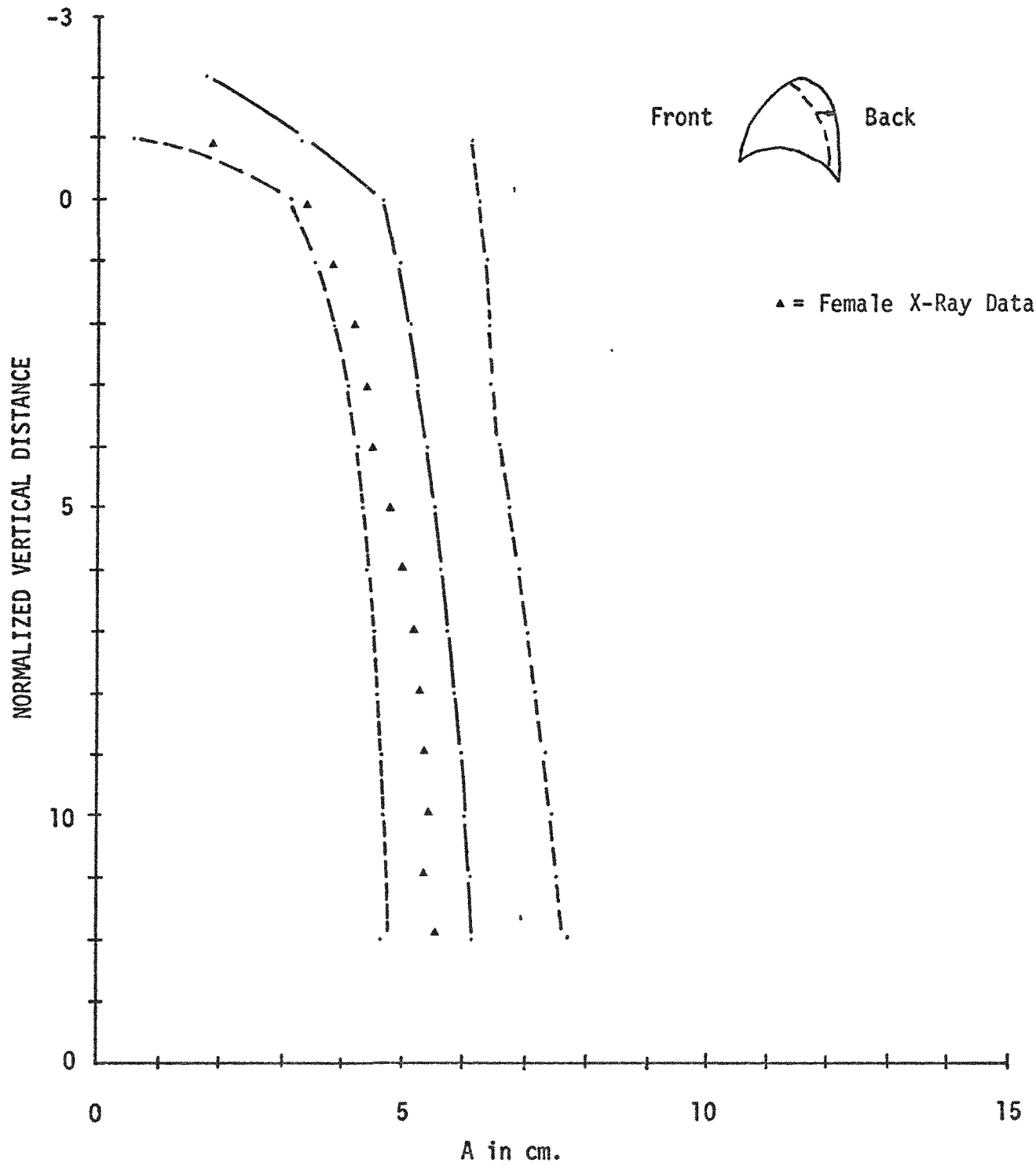
DORSAL DIMENSION (A), SIDE VIEW
AVG. ± 2 ST. DEV.
-3
0
5
10
0
NORMALIZED VERTICAL DISTANCE
Front
Back
▲ = Female X-Ray Data
0
5
10
15
A in cm.

FIGURE 19

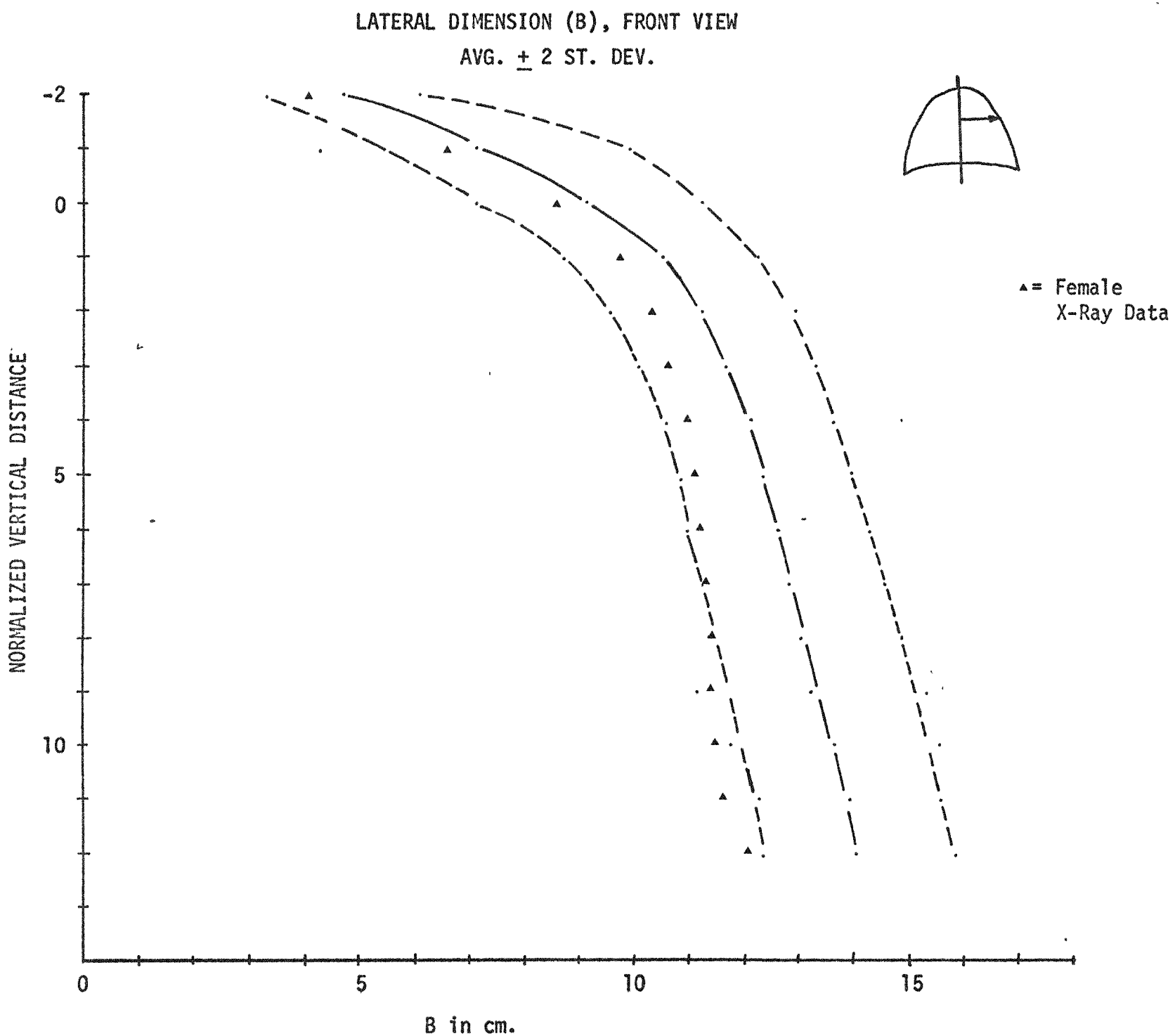
LATERAL DIMENSION (B), FRONT VIEW
AVG. ± 2 ST. DEV.
NORMALIZED VERTICAL DISTANCE
-2
0
5
10
0
5
10
15
B in cm.
▲= Female
X-Ray Data

FIGURE 20

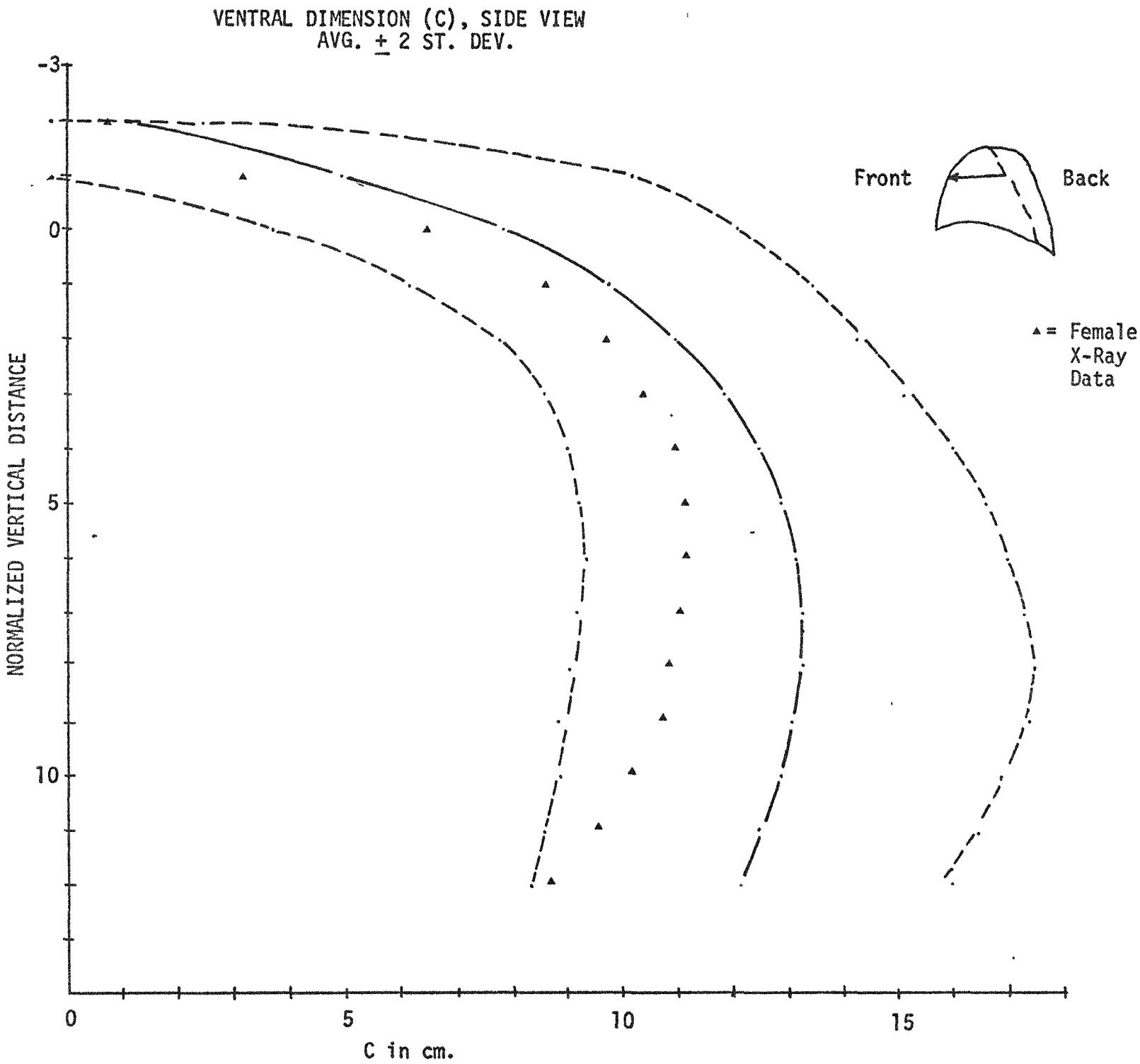
VENTRAL DIMENSION (C), SIDE VIEW
AVG. ± 2 ST. DEV.
-3
0
5
10
NORMALIZED VERTICAL DISTANCE
Front
Back
▲= Female X-Ray Data
0
5
10
15
C in cm.

FIGURE 21

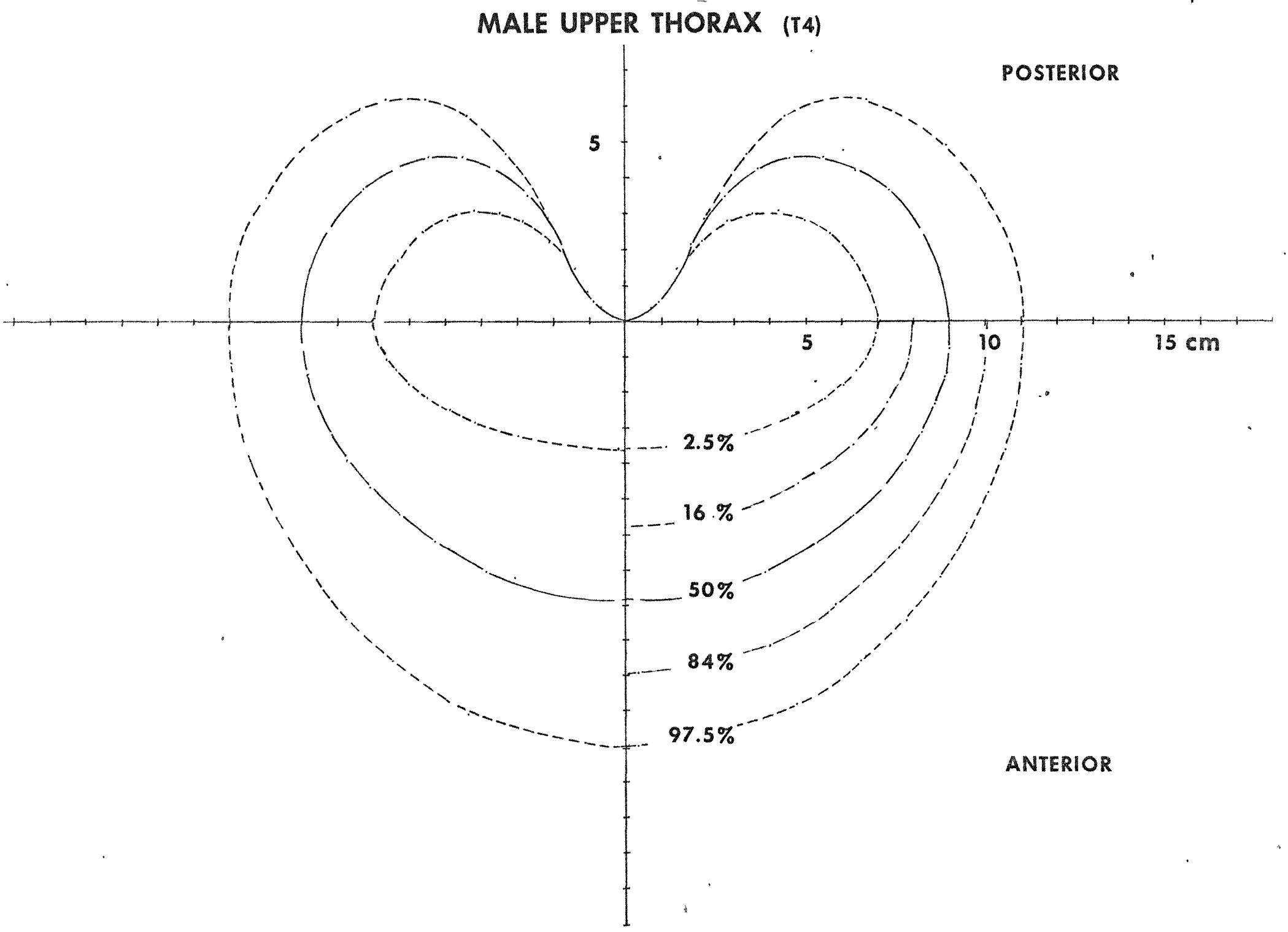
MALE UPPER THORAX (T4)
POSTERIOR
5
5
10
15 cm
2.5%
16 %
50%
84%
97.5%
ANTERIOR

FIG 22

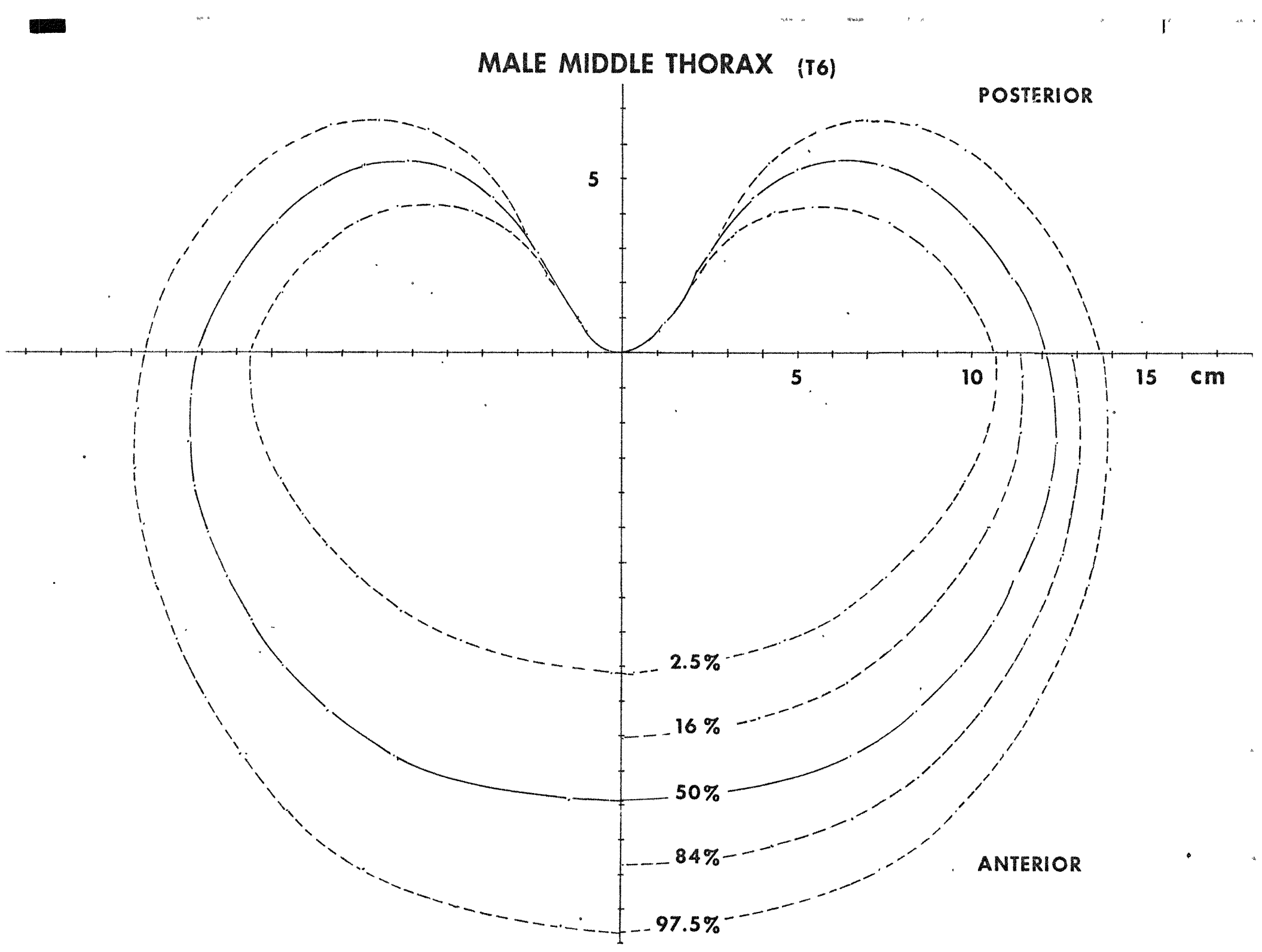
MALE MIDDLE THORAX (T6)
POSTERIOR
5
5
10
15
cm
2.5%
16%
50%
84%
97.5%
ANTERIOR

FIG 23

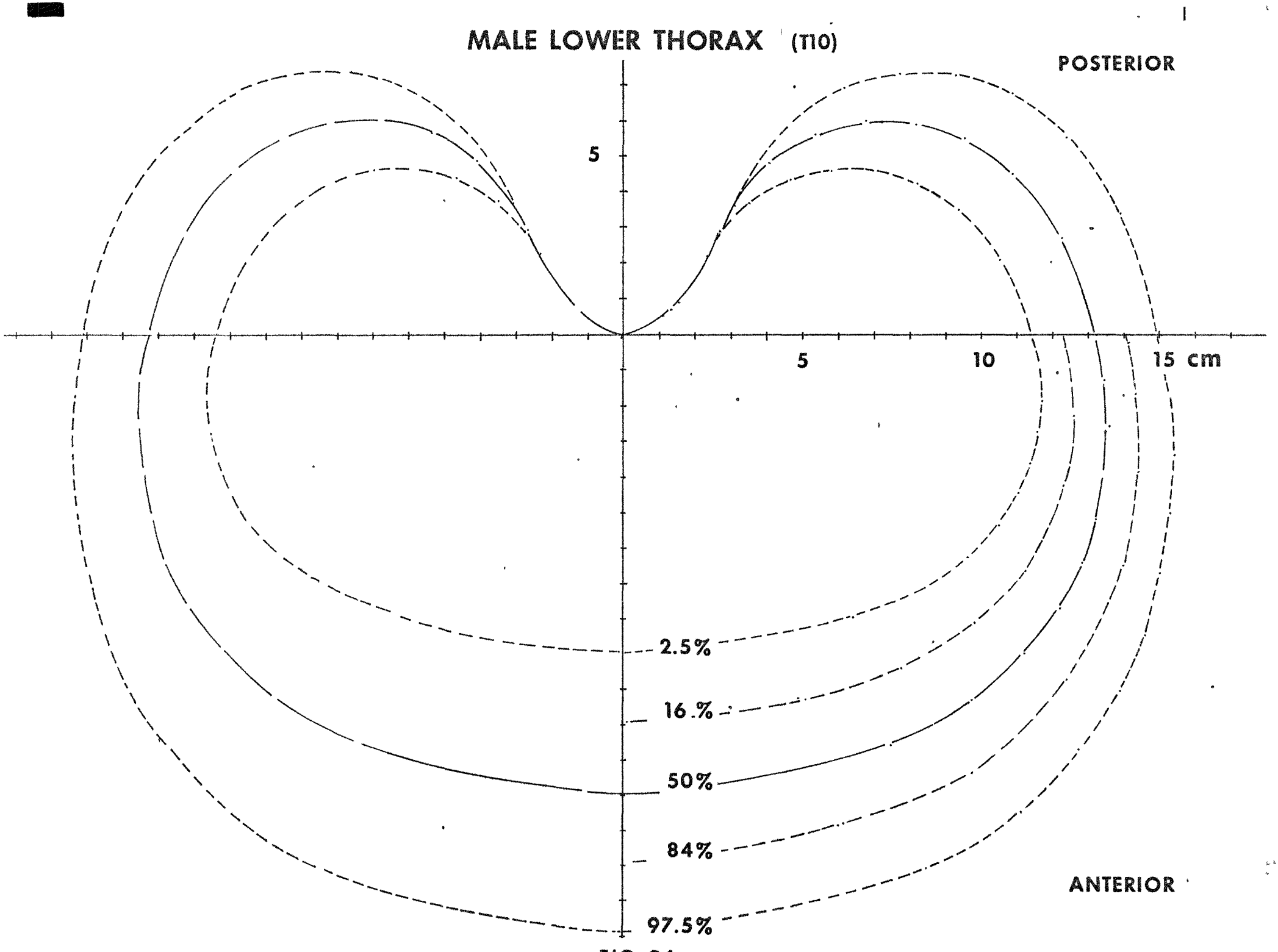
MALE LOWER THORAX (T10)
POSTERIOR
5
5
10
15 cm
2.5%
16.%
50%
84%
97.5%
ANTERIOR

FIG 24

x-ray data to predict a statistical thorax size distribution. Two more molds are expected. When these arrive, the model will be updated and finalized. Also, variability in shape between endomorph's, ectomorph's, etc. is under investigation.

3.2 ANATOMICAL AND PHYSIOLOGICAL TOLERANCE OF THE THERMAL CONVERTER IN CALVES

The AEC totally implantable artificial heart is composed of two independent parts -- the blood pump and the thermal converter.

A report on the initiation of the experimental study to locate acceptable spaces for the thermal converter was included in the last progress report (COO-2208-3), and this effort has been continued since then.

The intrathoracic cavity, the extraperitoneal intrapelvic space, the subcutaneous anterosternal space, and the retrovertebral space were discussed in detail in the last report with recommendation that these not be considered.

Actual implantations of the thermal converter model were performed in calves during the period of July and August of 1972. This report presents experimental results of the implantation obtained by physico-clinical examination, hemato-biochemical examination, and autopsy findings. Experimental materials, methods, animals and operative procedures were described in detail in the last report, and will be mentioned briefly in this report.

3.2.1 Materials and Methods

Thermal Converter Model. A Silastic* reproduction of the converter supplied by the AEC having a volume of 820 cm^3 and a weight of 1200 gm was made for implantation.

---

*Silastic RTV + Catalyst 4 from Dow Corning Corporation, Midland, Michigan.

Experimental Animals. Calves weighing about 80 kg each were used for these experiments.

Localization & Operative Procedure of the Implantation. The duplicate model was implanted in the extrapleural subcostal, in the retroperitoneal infrarenal, or in the intraperitoneal space. The implantations performed are tabulated in Table 7.

3.2.2 Results

Case 1 (Extrapleural Subcostal Implantation) and Case 2 (Retroperitoneal Infrarenal Implantation) were reported in the last progress report to have been in perfect condition after implantation and to be normal on physical, biochemical, and histological examinations at the eighth month after implantation at which time they were sacrificed.

Case 3 (Retroperitoneal Infrarenal Implantation)

Physico-clinical Examination. The animal recovered from the operation without any difficulty and has grown to over 300 kg in weight. The animal was in perfect condition 11-1/2 months after the implantation. The mold seemed to be wrapped by surrounding tissues and was not palpable over the skin.

Hematological and Biochemical Examination. Blood was sampled immediately before sacrifice for autopsy at 11-1/2 months after implantation. The data showed no particular changes in routine hematology, kidney and liver function (Table 8).

Autopsy Findings and Histological Examinations. The animal was sacrificed with intravenous administration of KCl solution. The mold was found positioned in the right retroperitoneal infrarenal space. It protruded into the abdominal cavity with the wide base adhering firmly

TABLE 7

LOCALIZATION OF IMPLANTATION, IDENTIFICATION OF THERMAL CONVERTER MODEL, AND PROGNOSIS OF CALVES

Calf No.	Implantation Site	Thermal Converter Model	Prognosis
1	Extrapleural, subcostal	S-S-D	Sacrificed for autopsy (8 months)
2	Retroperitoneal, infrarenal	S-S-D	Sacrified for autopsy (8 months)
3	Retroperitoneal, infrarenal	S-S & W-D	Sacrificed for autopsy (11-1/2 months)
4	Intraperitoneal	S-S & W-D	Sacrificed for autopsy (9-1/2 months)
5	Retroperitoneal, infrarenal	S-S & W-D	Still alive under observation (12 months)

S-S-D: Duplicating the size and the shape of the original.

S-S & W-D: Duplicating the size, the shape, and the weight of the original.

TABLE 8

HEMATOLOGY AND BLOOD BIOCHEMISTRY OF CASE 3

	8 Months After Implantation	11-1/2 Months After Implantation
Hematology:		
RBC	5.27×10^6	5.89×10^6
WBC	10.4×10^3	8.3×10^3
Hgb	9.0 g%	10.4 g%
Hct	22.6%	24.7%
Platelet	4.00×10^5	3.89×10^5
Serum Protein Fraction:		
Albumin	52%	
α-globulin	13%	
β-globulin	18%	
γ-globulin	18%	
Blood Chemistry:		
T.P.	6.7 gm%	7.2 gm%
BUN	0.7 mg%	7.0 mg%
Creatinine	1.1 mg%	1.2 mg%
Alk. Phos.	12.1 KAU	9.5 KAU
T. Bilirubin	0.7 mg%	0.7 mg%
Cholesterol	113 mg%	105 mg%
Glucose	52 mg%	75 mg%
Na^+	141 mEq/L	145 mEq/L
K^+	4.0 mEq/L	4.2 mEq/L
Cl^-	98 mEq/L	98 mEq/L
Ca^{++}	9.1 mg%	9.2 mg%

with the right kidney and with the free apex toward the intraperitoneal cavity. The whole mold was encapsulated by thick fibrous connective tissues and was completely isolated from the other organs. No signs of inflammation were noticed. There was no detectable macroscopic abnormality in the internal organs (Table 9, Figure 25). Microscopic examination indicated no abnormality.

Case 4 (Intraperitoneal Implantation)

Physico-clinical Examination. The animal had been doing well after operation. The mold, which had migrated and positioned itself at the lowest level in the intraperitoneal cavity immediately after completion of the operation, was not palpated over the skin.

Hematological and Biochemical Examination. Blood was sampled immediately before sacrifice for autopsy at 9-1/2 months after implantation. Hematology data were normal. Serum protein fraction was properly balanced. Blood chemistry showed no kidney or liver dysfunction (Table 10).

Autopsy Findings and Histological Examinations. The animal was sacrificed with KCl solution. The abdomen was opened through a midline incision and the stomachs were exteriorized outside the body. Then, the mold appeared completely encapsulated with a thin fibrous sheath which adhered to the right colon. The mold appeared to be fixed by surrounding tissues still keeping some extent of freedom of mobilization. The encapsulated mold was easily taken apart from surrounding tissues. There was no noticeable macroscopic changes in any internal organs. Microscopic examination reported no particular changes (Table 11, Figure 26).

Case 5 (Retroperitoneal Infrarenal Implantation)

TABLE 9

WEIGHT OF ORGANS OF CASE 3 AT AUTOPSY

Brain		60 gm
Heart		620 gm
Lung:	Right	760 gm
	Left	600 gm
Liver		2800 gm
Spleen		120 gm
Kidney:	Right	200 gm
	Left	140 gm

TABLE 10

HEMATOLOGY AND BLOOD BIOCHEMISTRY OF CASE 4

	9-1/2 Months After Implantation
Hematology:	
RBC	5.75×10^6
WBC	5.6×10^3
Hgb	9.3 gm%
Hct	24.9%
Platelet	1.35×10^5
Serum Protein Fraction:	
Albumin	48%
α-globulin	17%
β-globulin	15%
γ-globulin	20%
Blood Chemistry:	
T.P	5.7 gm%
BUN	5.0 mg%
Creatinine	1.0 mg%
Alk. Phos.	31 KAU
T. Bilirubin	0.3 mg%
Cholesterol	90 mg%
Glucose	63 mg%
Na+	138 mEq/L
K+	4.7 mEq/L
Cl-	100 mEq/L
Ca++	11.5 mEq.L

TABLE 11

WEIGHT OF ORGANS OF CASE 4 AT AUTOPSY

Brain	340 gm
Heart	970 gm
Lung: Right	1000 gm
Left	740 gm
Liver	2820 gm (including gallbladder)
Spleen	300 gm
Kidney: Right	370 gm
Left	390 gm
Adrenal: Right	10 gm
Left	10 gm
Mold Capsule	130 gm; 0.3 cm thick

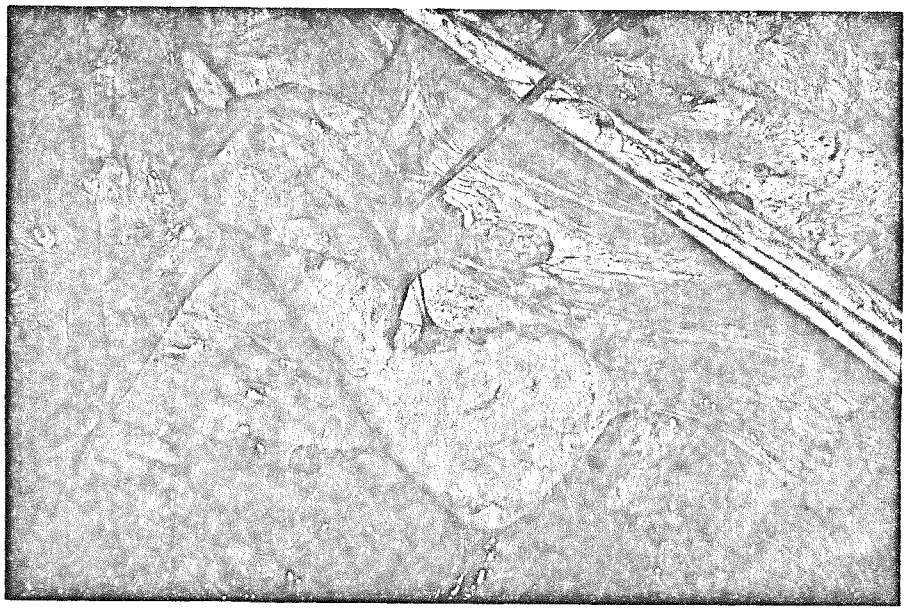

FIGURE 25

AUTOPSY OF CASE 3 (RETROPERITONEAL INFRARENAL IMPLANTATION)

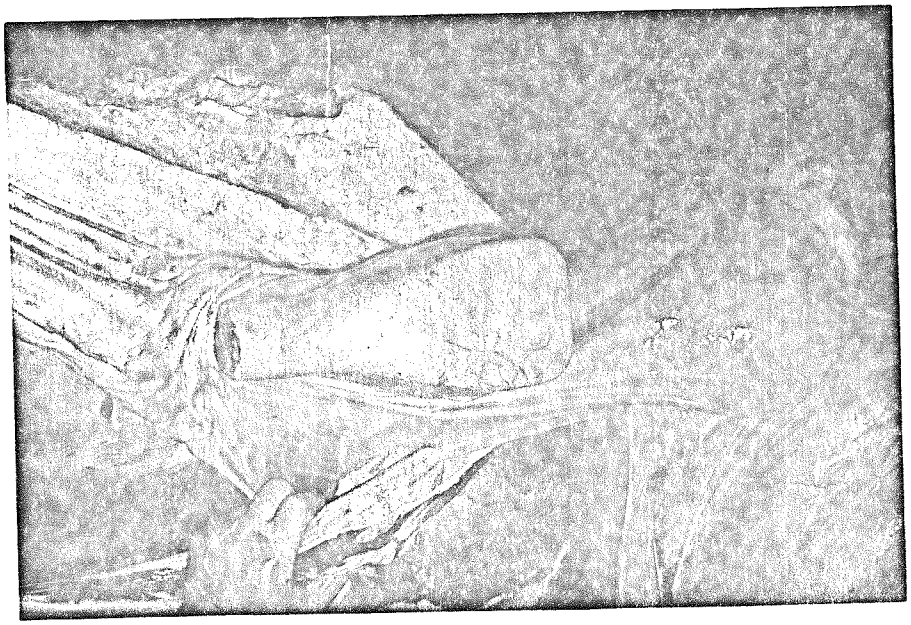

FIGURE 26

AUTOPSY OF CASE 4 (INTRAPERITONEAL IMPLANTATION)

There has been no difficulty during the course of convalescence after surgery. The animal has grown to over 350 kg and has been on periodic examinations.

3.2.3 Discussion and Conclusions

The implantation in the retroperitoneal infrarenal or in the intraperitoneal space did not cause any physical disorders, which was also supported by hematological, biochemical and histological examinations. It is interesting to indicate that serum protein fraction has been kept within normal ranges in all experimental animals even with the Silastic molds implanted. This probably suggests that the Silastic is inert enough to the living body as a covering material of the artificial heart.

In conclusion, all the spaces examined appear tolerable for converter implantation as far as space availability is concerned. However, considering secure and safe anchoring of the unit to the hard structure, the vertebral column, and minimal possible sacrifice of function of the internal organs, the retroperitoneal infrarenal space is still thought to be most preferable for thermal converter implantation.

APPENDIX A

RADIOGRAPH MEASUREMENT TECHNIQUE

MEASUREMENTS ON POSTERO-ANTERIOR RADIOGRAPHS (Fig. 7):

1. Define the median line (I), assuming that the chest is symmetric.

2. Locate the fourth and tenth ribs of both sides.

3. Draw the lines, which cross perpendicularly to (I) and pass through the points at which the fourth (II) and tenth rib (III) is farthest from line (I).

4. Draw a line from the mid-point of Line II, parallel to (I), to Point (IV) on the dorsal shadow of the fourth rib. Do the same and obtain Point (V) on the tenth rib.

5. Define the upper reference point (P_0) on Line (I) where a line perpendicular to Line (I) passes through Point (IV). Define the lower reference point (P_{10}) on Line (I) from Point (V).

6. Measure the distance between Point (P_0) and (P_{10}). This is Vmax.

7. Divide Vmax into ten divisions and name divisional points in an order of P_0, P_1, P_2 .... P_{10} and extend these points on Line (I) upward to P_1, P_2 .... and downward to P_{11}, P_{12} with the same divisional distance.

8. Measure distances B_0, B_1, B_2 .... B_{10} and B_{-1}, B_{-2} .... B_{11}, B_{12} .... as many as exist in such a manner as B_n is a distance between Point (P_n) and a point at which a perpendicular to Line (I), passing through P_n, crosses the internal margin of the chest cavity on a radiograph.

9. Measure distances D_0, D_1, D_2 .... which are defined by the distances from P_0, P_1, P_2 .... to points at which lines perpendicular

to Line (I) and passing through P_0, P_1, P_2 ... cross the right margin of the heart silhouette.

10. Measure distances E_0, E_1, E_2 ... which are defined as the same as D_0, D_1, D_2 ...., but to the left margin of the heart silhouette. An upper and lower limitation of the pericardial cavity are confirmed on a corresponding lateral view of chest radiograph.

If any upper and/or lower limitation of structures to be measured are not on exact divisions, half the divisional scale is set and indicated on a chart. (For example (3.5) in Column D in Table 1). The level of each side of the diaphragm is individually noted in Table 12 since very often it differs.

MEASUREMENTS ON LATERAL RADIOGRAPHS (Figure 8):

1. Locate and define the reference point (Q_0) on the anterior line of the vertebral column which has already been determined as the corresponding point (P_0) on a posteroanterior view. Point ($P_0 = Q_0$) usually positions itself at a lower rim of the third thoracic vertebra.

2. Define Point (R_0) which is marked on a posterior edge of the film and at the same horizontal level to (Q_0).

3. Make Point (R_{10}) on a posterior edge of the film with a distance of Vmax from R_0. Q_{10} can be marked by tracing a horizontal line passing through R_{10} on the anterior line of the vertebral column.

4. Divide the distance between R_0 and R_{10} into ten divisions and name divisional points in an order of R_0, R_1, R_2 .... R_{10} and extend these points upward to R_{-1}, R_{-2} .... and downward to R_{11}, R_{12} .... with the same divisional distance.

5. Mark Q_1, Q_2 .... Q_9 on the anterior line of the vertebral column so as to be at the same horizontal level to the corresponding points of R_1, R_2 .... R_9.

6. Measure distances C_0, C_1 .... C_{10} in such a manner as C_n is defined by a horizontal distance between Q_n and the anterior internal margin of the chest cavity.

7. Measure distances A_0, A_1 ... A_{10} and A_{-1}, A_{-2} ... A_{-11}, A_{-12} ... in such a manner as A_n is defined by a horizontal distance between Q_n and the posterior internal margin of the chest cavity.

8. Measure distances .... F_2, F_3 .... F_5, F_6 .... in such a manner as F_n is defined by a distance between Q_n and the point where a horizontal line through Q_n crosses an anterior line of the heart silhouette.

9. Measure distances .... G_2, G_3 .... G_5, G_6 ... in such a manner as G_n is defined by a distance between Q_n and the point where a horizontal line through Q_n crosses a posterior line of the heart silhouette. A typical case of the measurements is presented in Table 12.

TABLE 12

NO. 74 NAME: B.J.R. SEX: Male
AGE: 54

	A	B	C	D	E	F	G
-5							
-4							
-3							
-2		(-1.5) 4.4	(-1.5) 0.5				
-1	3.0	6.8	8.0				
0	5.0	9.6	10.1				
1	5.4	11.6	13.2				
2	5.6	12.7	13.6				
3	5.8	13.3	13.6	(3.5) 2.0	(3.5) 2.2	(3.5) 7.8	(3.5) 7.8
4	6.1	14.0	13.8	2.6	2.2	10.8	6.5
5	6.5	14.1	13.5	3.0	2.4	12.5	4.1
6	7.2	14.6	13.2	3.4	3.1	13.2	3.1
7	7.5	14.7	12.9	3.6	4.2	12.9	2.8
8	7.5	14.8	12.5	4.3	6.1	12.5	2.5
9	7.6	14.8	12.4	4.5	8.0	12.4	2.5
10	7.6	15.4	12.4	4.5	9.0	12.4	3.2
11	7.6	15.4	12.4	4.5	10.0	12.4	5.0
12	7.6	R L (12.0) (12.0) 9.0 11.0	R L (12.0) (12.0) 7.0 7.0	4.5	10.5		
13							
14							
15							
16							
Vmax	18.0						

( ) indicates a divisional scale.

Numbers indicate actual distance in cm.